

Margin-aware Preference Optimization for Aligning Diffusion Models without Reference

Jiwoo Hong^{*†} Sayak Paul^{*‡} Noah Lee[†] Kashif Rasul[‡]
 James Thorne[†] Jongheon Jeong[§]

[†]KAIST AI [‡]Hugging Face [§]Korea University

Abstract

Modern alignment techniques based on human preferences, such as RLHF and DPO, typically employ divergence regularization relative to the reference model to ensure training stability. However, this often limits the flexibility of models during alignment, especially when there is a clear distributional discrepancy between the preference data and the reference model. In this paper, we focus on the alignment of recent text-to-image diffusion models, such as Stable Diffusion XL (SDXL), and find that this “reference mismatch” is indeed a significant problem in aligning these models due to the unstructured nature of visual modalities: e.g., a preference for a particular stylistic aspect can easily induce such a discrepancy. Motivated by this observation, we propose a novel and memory-friendly preference alignment method for diffusion models that does not depend on any reference model, coined *margin-aware preference optimization* (**MaPO**). MaPO jointly maximizes the likelihood margin between the preferred and dispreferred image sets and the likelihood of the preferred sets, simultaneously learning general stylistic features and preferences. For evaluation, we introduce two new pairwise preference datasets, which comprise self-generated image pairs from SDXL, *Pick-Style* and *Pick-Safety*, simulating diverse scenarios of reference mismatch. Our experiments validate that MaPO can significantly improve alignment on Pick-Style and Pick-Safety and general preference alignment when used with Pick-a-Pic v2, surpassing the base SDXL and other existing methods. Our code, models, and datasets are publicly available via <https://mapo-t2i.github.io>.

Warning: This paper contains examples of harmful content, including explicit text and images.



Figure 1: Stable Diffusion XL trained with **MaPO**. MaPO simultaneously adapts the text-to-image diffusion model to desired styles and aligns the model to human preference without reference model.

^{*}Equal contribution.

[†]{jiwoo_hong,noah.lee,thorne}@kaist.ac.kr [‡]{sayak,kashif}@huggingface.co [§]jonghj@korea.ac.kr

Stable Diffusion XL (Base Model)

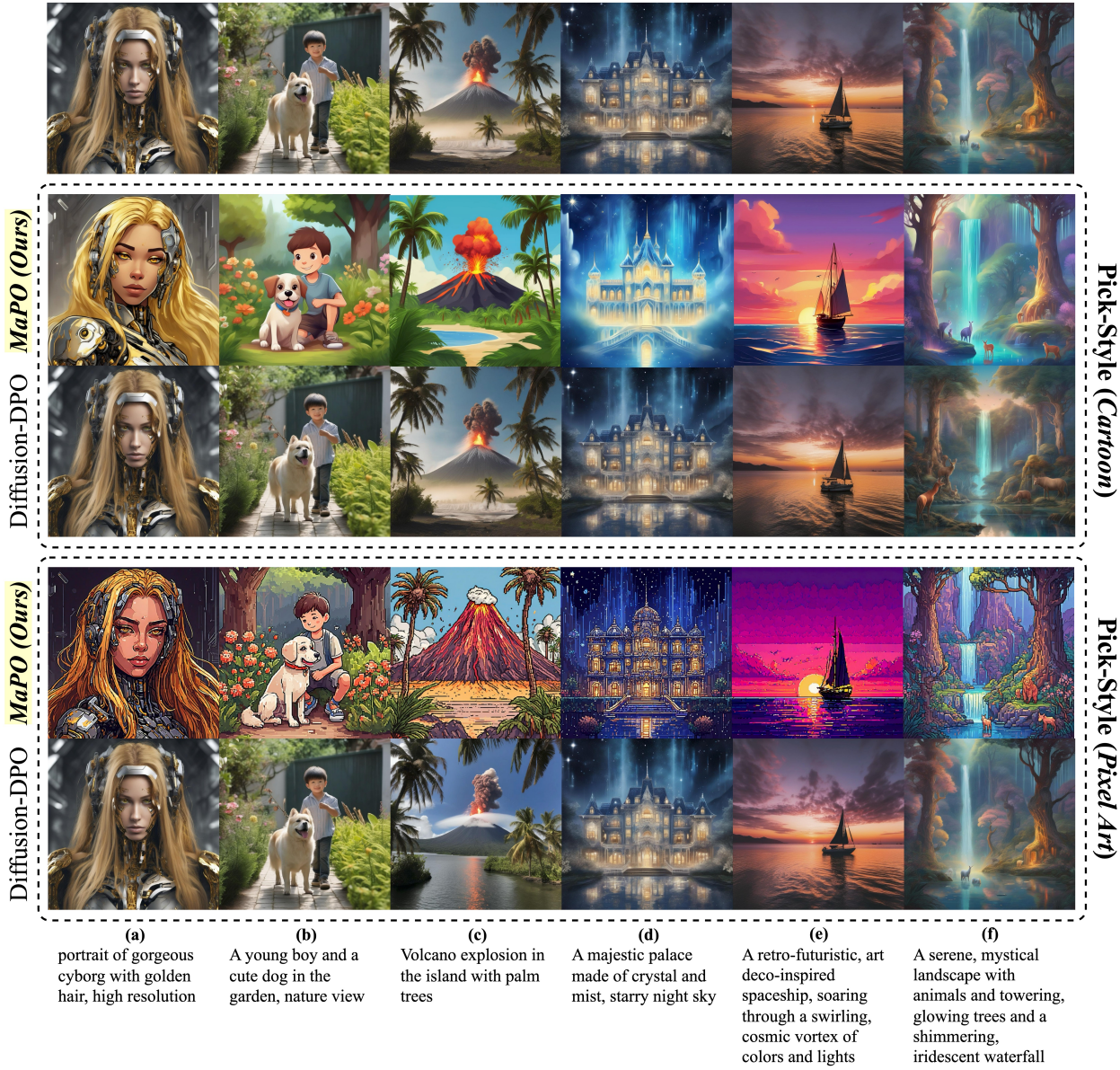


Figure 2: Stable Diffusion XL (SDXL) trained with **MaPO** and Diffusion-DPO on Pick-Style cartoon (middle) and pixel art (bottom) split. When the preference dataset has distinct styles from the base model, Diffusion-DPO fails to induce such styles, while MaPO successfully induces both the stylistic feature and the preference.

1 Introduction

Diffusion models have become a dominant framework for modeling high-dimensional data distributions thanks to their scalability [Ho et al., 2020, Kingma et al., 2021, Rombach et al., 2022, Podell et al., 2024, Peebles and Xie, 2023, Esser et al., 2024], and have been successfully applied to many large-scale generative modeling tasks combined with diverse conditioning: *viz.*, text [Li et al., 2022, Strudel et al., 2022], images [Ho et al., 2020, Podell et al., 2024], and audio [Kong et al., 2021, Evans et al., 2024]. As their capabilities increase and extend across modalities, diffusion models are being applied to a wider range of human-centered applications, which has motivated practitioners to consider *fine-tuning* of these models for better alignment with human preferences, with respect to various values such as safety [Shen et al., 2024, Schramowski et al., 2023], styles [Hertz et al., 2024], and personalization [Ruiz et al., 2023, von Rütte et al., 2023], to name a few.

Aligning text-to-image diffusion models aims to elicit desired styles of generations given the prompt via fine-tuning, particularly using recent *preference optimization* techniques [Lee et al., 2023, Yoon et al., 2023, Fan et al., 2023, Wallace et al., 2023, Li et al., 2024c, Yuan et al., 2024]. For example, methods based on reinforcement learning (RL) [Fan et al., 2023, Black et al., 2024] view denoising diffusion as a multi-step decision-making process and maximize an auxiliary feedback-trained reward, *e.g.*, via proximal policy optimization [Schulman et al., 2017]. A common practice adopted by these methods, whether based on RL or not, is the use of a *reference model* during optimization for training stability. Specifically, they typically introduce a divergence regularization to the reference model as a prior to prevent fine-tuning from overfitting to the limited preference data, which could result in losing core generative abilities or “hacking” the reward model [Ziegler et al., 2020, Wang et al., 2024a, Skalse et al., 2022, Pang et al., 2023].

However, enforcing a model to be close to a certain reference can rather limit the flexibility in learning new content [Tajwar et al., 2024], especially when the reference model and preference data have distinct features, a situation we refer to as *reference mismatch*. The significance of reference mismatch has been empirically demonstrated when aligning large language models (LLMs). For instance, Tunstall et al. [2023] have shown that aligning a pre-trained LLM on domain-specific preference pairs, *i.e.*, without extensive supervised fine-tuning (SFT) to match the domain, can deteriorate the resulting model. In the context of text-to-image models, reference mismatch can occur due to various reasons. For example, a specific preference for a certain style, such as pixel art, can create a mismatch, or a limited sample size in personalization can also induce an implicit distributional bias. Yet, addressing such distributional discrepancies during preference optimization of text-to-image diffusion models remains under-explored, demanding further research.

Contribution. We focus on the limitation of existing preference optimization methods that leverage reference models for aligning text-to-image diffusion models. Specifically, we show that the reference model can impede preference optimization under distributional discrepancy (*i.e.*, reference mismatch) between the preference data and those represented by the reference model. To this end, we introduce two new self-curated preference datasets: *Pick-Style* and *Pick-Safety*, as depicted in Figure 3. By taking a closer look at the role of the reference model in Diffusion-DPO [Wallace et al., 2023], we categorize reference mismatch into two cases by which side of preference data (*i.e.*, either preferred or dispreferred) specifically incurs the distributional mismatch. Our empirical results underscore that neither Diffusion-DPO nor SFT can adapt the diffusion model to the preference with disparate stylistic properties, as shown in qualitative samples in Figure 2.

Motivated by the observation, we present *margin-aware preference optimization* (MaPO), a novel preference optimization method for aligning text-to-image diffusion models that do not depend on any reference model. MaPO replaces divergence regularization on the reference model in Diffusion-DPO with an amplification factor defined by the trained policy’s likelihood estimation, being free from the reference mismatch. Our analysis demonstrates that the gradient of MaPO leads to stronger adaptation toward the preferred styles along with weak penalty to the dispreferred styles in comparison to SFT, as in Figure 3.

We demonstrate the effectiveness of MaPO with an extensive empirical evaluation, both in quantitative and qualitative manners. With an automatic evaluation based on GPT-4o, we show that MaPO achieves at least 73% win rate against Diffusion-DPO and SFT in adapting on Pick-Style and Pick-Safety datasets we introduce, confirming that MaPO is more flexible under reference mismatch. Furthermore, we report that MaPO adapted on Pick-a-Pic v2 [Kirstain et al., 2023] for general human preference alignment could outperform or match 21 out of 25 state-of-the-art text-to-image diffusion models in ImgSys public benchmark [Taskaya et al., 2024]: our anonymously entered model significantly outperforms the Diffusion-DPO entry from the same Pick-a-Pic v2, *e.g.*, 7th (of MaPO) vs. 20th (of Diffusion-DPO) place on the leaderboard at the time of writing, while also consuming 14.5% less wall-clock training time. Lastly, we also show the versatility of MaPO in alignment and aesthetics with various static metrics, including Aesthetics [Schuhmann, 2023], HPS v2.1 [Wu et al., 2023a], and Pick-Score [Kirstain et al., 2023], reporting consistent gains upon the base Stable Diffusion XL [Podell et al., 2024].

2 Preliminaries

Text-to-image diffusion models. A text-to-image diffusion model [Rombach et al., 2022, Saharia et al., 2022, Ramesh et al., 2022] learns to denoise random noise $x_T \sim N(0, \mathbf{I})$ towards a data distribution $x_0 \sim p_{\text{data}}(x_0)$ conditioned on textual prompts c . Specifically, it models a discrete Markov process $p_\theta(x_{t-1}|x_t, c)$ that predicts

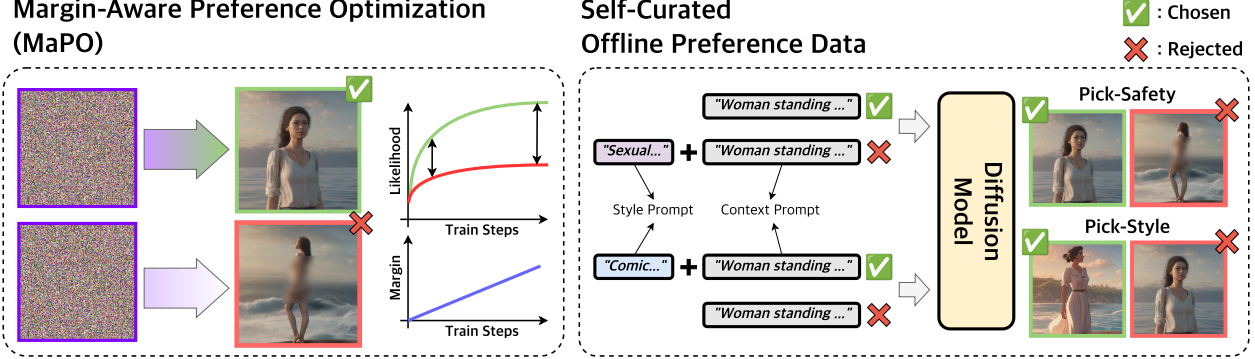


Figure 3: General diagram of margin-aware preference optimization (MaPO). MaPO effectively learns stylistic features and preferences regardless of the stylistic discrepancy. With self-curated offline preference data curated by prepending style-specific prompts, we simulate the reference mismatch by focusing on either a strong dispreferred style (Pick-Safety) or preferred style (Pick-Style).

x_{t-1} from x_t for timesteps $t = T, \dots, 1$, where x_t has the marginal distribution from the diffusion process:

$$q(x_t | x_0) = N(\alpha_t x_0, \sigma_t^2 \mathbf{I}), \quad (1)$$

with a certain noise scheduling of α_t and σ_t . Given $x_T \sim N(0, \mathbf{I})$, the backward denoising process, or “denoising” process, of text-to-image diffusion model is defined as the following:

$$p_\theta(x_{0:T} | c) = \prod_{t=1}^T p_\theta(x_{t-1} | x_t, c). \quad (2)$$

In order to maximize the likelihood of $p_\theta(x_0 | c)$ with respect to $p_{\text{data}}(x_0)$, the evidence lower bound (ELBO) across T backward processes is minimized. In a nutshell, Ho et al. [2020, DDPM] have proposed to parameterize p_θ as a noise predictor $\epsilon_\theta(x_t, c, t)$, which results in the following mean squared error (MSE) based objective from random noise $\epsilon \sim N(0, \mathbf{I})$:

$$\mathcal{L}_{\text{DDPM}} := \mathbb{E}_{x_T} [-\log p_\theta(x_0, c)] \leq T \cdot \mathbb{E}_{x_0, \epsilon, t} \left[\omega(\lambda_t) \left\| \epsilon - \epsilon_\theta \left(\sqrt{\bar{\alpha}_t} x_0 + \sqrt{1 - \bar{\alpha}_t} \epsilon, c, t \right) \right\|^2 \right], \quad (3)$$

where $\omega(\lambda_t)$ are constants dependent on the signal-to-noise ratio $\lambda_t = \log(\alpha_t^2 / \sigma_t^2)$ of noise scheduling [Song and Ermon, 2019, Kingma et al., 2021] and $\bar{\alpha}_t$ is a product of α_t up to timestep t [Ho et al., 2020]. In practice, Ho et al. [2020] have further considered a simplified loss that ignores $\omega(\lambda_t)$:

$$\mathcal{L}_{\text{Simple}}(c, x_0; \theta) := \mathbb{E}_{\epsilon, t} \left[\left\| \epsilon - \epsilon_\theta \left(\sqrt{\bar{\alpha}_t} x_0 + \sqrt{1 - \bar{\alpha}_t} \epsilon, c, t \right) \right\|^2 \right]. \quad (4)$$

Aligning via preference optimization. Aligning a generative model typically refers to fine-tuning the model to generate outputs that are more preferable to humans [Ouyang et al., 2022]. Human preferences are often acquired as a preference pair (x^w, x^l) given a prompt c , where x^w (“chosen”) is more preferred than x^l (“rejected”) by a human annotator. Such preference data can be used for modeling $p(x^w > x^l | c)$, which is referred as the Bradley-Terry model [Bradley and Terry, 1952]:

$$p(x^w > x^l | c) = \frac{\exp(r(x^w, c))}{\exp(r(x^w, c)) + \exp(r(x^l, c))}, \quad (5)$$

where $r(x, c)$ denotes a reward function given a prompt c and its output x . This preference modeling has been popularized in aligning large language models [Ziegler et al., 2020, Rafailov et al., 2023], especially combined with reinforcement learning (RL) techniques such as proximal policy optimization [Schulman

et al., 2017, PPO] to fine-tune the model based on the learned reward from human preferences, *viz.*, *RL from human feedback* (RLHF). More specifically, RLHF optimizes a model p_θ to maximize the following objective given a reward $r(x, c)$:

$$\max_{p_\theta} \mathbb{E}_{c, x \sim p_\theta(x|c)} [r(x, c)] - \beta \cdot \mathbb{D}_{\text{KL}}(p_\theta(x | c) \| p_{\text{ref}}(x | c)), \quad (6)$$

where p_{ref} is a *reference model*, typically set by p_θ at the initial (pre-trained) weights, to prevent p_θ from drifting too much during the optimization. It can be shown that the objective in Equation (6) converges to the following policy model:

$$p^*(x | c) = \frac{1}{Z(c)} p_{\text{ref}}(x | c) \exp \left(\frac{1}{\beta} \cdot r(x, c) \right), \quad (7)$$

where Z is the partition function. Motivated by this, Rafailov et al. [2023, DPO] have derived a training objective for p_θ that is equivalent to Equation (7) but without requiring explicit $r(x, c)$: it rather learns directly from the preference data $(c, x^w, x^l) \sim D$.

$$\mathcal{L}_{\text{DPO}}(\theta; p_{\text{ref}}) = -\mathbb{E}_{(c, x^w, x^l) \sim D} \left[\log \sigma \left(\beta \cdot \log \frac{p_\theta(x^w | c)}{p_{\text{ref}}(x^w | c)} - \beta \cdot \log \frac{p_\theta(x^l | c)}{p_{\text{ref}}(x^l | c)} \right) \right], \quad (8)$$

where $\sigma(\cdot)$ denotes the sigmoid function.

In the context of aligning text-to-image models, recent works [Wallace et al., 2023, Yoon et al., 2023, Fan et al., 2023, Li et al., 2024c] have been actively revisiting the ideas of preference optimization, particularly for diffusion models. For example, Wallace et al. [2023, Diffusion-DPO] have proposed an adaptation of DPO in diffusion fine-tuning by considering preferences over *diffusion paths*, namely in terms of $x_{1:T}^w$ and $x_{1:T}^l$:

$$\mathcal{L}_{\text{Diff-DPO}}(\theta; p_{\text{ref}}) = -\mathbb{E}_{c, x_0^l, x_0^w} \left[\log \sigma \left(\beta \mathbb{E}_{x_{1:T}^l, x_{1:T}^w} \left[\log \frac{p_\theta(x^w | c)}{p_{\text{ref}}(x^w | c)} - \log \frac{p_\theta(x^l | c)}{p_{\text{ref}}(x^l | c)} \right] \right) \right]. \quad (9)$$

3 Margin-aware Preference Optimization for Diffusion Models

This section focuses on the issue of *reference mismatch* in aligning text-to-image diffusion models. We first discuss specific situations of reference mismatch and their potential impacts on text-to-image diffusion models in Section 3.1. On top of it, through Sections 3.2 and 3.3, we propose a novel alignment method for diffusion models, *margin-aware preference optimization* (MaPO), that aims to mitigate the issue by eliminating the need for reference model during preference optimization.

3.1 Reference mismatch when aligning diffusion models

Reference mismatch, a significant distributional discrepancy between the reference model p_{ref} and a binary preference dataset $(c, x_0^l, x_0^w) \sim D$, disrupts stable and optimal preference optimization for the methods leveraging reference model [Tajwar et al., 2024].

By aligning the text-to-image diffusion model $p_\theta(x_0 | c)$ to the binary preference dataset $(c, x_0^l, x_0^w) \sim D$, the resulting model $p(x_0 | c)$ is expected to assign higher likelihood for x_0^w than x_0^l given the prompt c throughout the denoising process over T steps as in:

$$\mathbb{E}_{(c, x^l, x^w) \sim D} [\log p(x_{1:T}^w | c)] > \mathbb{E}_{(c, x^l, x^w) \sim D} [\log p(x_{1:T}^l | c)], \quad (10)$$

so that the prompt c would lead to $p(x_0 | c)$ generating a human-preferred image x_0^w . And with the loss function of Diffusion-DPO in Equation (9), minimizing $\mathcal{L}_{\text{Diff-DPO}}$ would lead to:

$$\mathbb{E}_{(c, x^l, x^w) \sim D} \left[\log \frac{p(x_{1:T}^w | c)}{p_{\text{ref}}(x_{1:T}^w | c)} \right] > \mathbb{E}_{(c, x^l, x^w) \sim D} \left[\log \frac{p(x_{1:T}^l | c)}{p_{\text{ref}}(x_{1:T}^l | c)} \right], \quad (11)$$

where the expected log-likelihood ratio of $p(x_0^w \mid c)$ and $p_{\text{ref}}(x_0^w \mid c)$ should be greater than that of x_0^l . By rearranging this, the log-likelihood for x_0^w should be greater than that of x_0^l with the specific margin defined by the KL divergence between $p_{\text{ref}}(x_{1:T}^w \mid c)$ and $p_{\text{ref}}(x_{1:T}^l \mid c)$:

$$\mathbb{E}_{(c, x^l, x^w) \sim D} \left[\log p(x_{1:T}^w \mid c) - \log p(x_{1:T}^l \mid c) \right] > \mathbb{E}_{(c, x^l, x^w) \sim D} \left[\log \frac{p_{\text{ref}}(x_{1:T}^w \mid c)}{p_{\text{ref}}(x_{1:T}^l \mid c)} \right]. \quad (12)$$

Here, such formulation could result in two situations by the direction of the right-hand side of Equation (12), which we name as *reference-chosen mismatch* and *reference-rejected mismatch*.

1. **Reference-chosen mismatch:** By $p_{\text{ref}}(x_{1:T}^w \mid c)$ being far *less* than $p_{\text{ref}}(x_{1:T}^l \mid c)$, the right-hand side of Equation (12) will consistently be negative over the given dataset. This could occur when the styles of *chosen* images are distant from the reference model; in such case, Equation (12) might not guarantee satisfying Equation (10). when the reference model does not have an understanding of latent preference shown in the given preference dataset.
2. **Reference-rejected mismatch:** By $p_{\text{ref}}(x_{1:T}^w \mid c)$ being far *greater* than $p_{\text{ref}}(x_{1:T}^l \mid c)$, the right-hand side of Equation (12) will consistently be positive throughout the given dataset. Equation (10) will be satisfied even before fine-tuning $p_\theta(x_0 \mid c)$, as it is initialized from $p_{\text{ref}}(x_0 \mid c)$. This indicates that the benefit of further alignment-tuning could be marginal, which is supported by the findings in aligning language models with DPO [Rafailov et al., 2023], where alignment after a fine-grained supervised fine-tuning (SFT) with high-quality data gave marginal or no improvements [Zhou et al., 2023, Sharma et al., 2024].

3.2 Benchmarking reference mismatch: Pick-Safety and Pick-Style

To empirically validate the efficacy of preference optimization methods in two reference mismatch scenarios, reference-rejected mismatch and reference-chosen mismatch, we introduce two new self-curated binary preference datasets based on Pick-a-Pic v2 [Kirstain et al., 2023] as shown in Figure 3: *Pick-Style* and *Pick-Safety*. We sample 1,000 instances from Pick-a-Pic v2 for both datasets and extract the context prompts that depict the core contexts using GPT-3.5-Turbo with the instructions in Appendix A. Then, we prepend the style prompt, which specifies a certain style choice, like cartoon or pixel art. With those prompts, we generate chosen and rejected images with Stable Diffusion XL [Rombach et al., 2022, SDXL].

1. **Pick-Style (Reference-chosen mismatch):** We make two splits of style-grounded preference dataset, cartoon and pixel art, by prepending “Disney style animated image.” and “Pixel art style image.”. Then, we prepend “Realistic 8k image.” to the context prompt for rejected images. Therefore, an ideally aligned model should generate the animated or pixel art images given the prompt, respectively. As stylistic prefixes make major changes in the *chosen* images, we intend to simulate the situation in which the reference model is distant from the chosen style.
2. **Pick-Safety (Reference-rejected mismatch):** We sampled the prompts with *women*, *woman*, *girl*, and *female* to build the safety-grounded preference dataset, Pick-Safety. We prepended “Sexual, nudity, +19 image.” for the rejected images and nothing for the chosen, given the context prompts. Thus, an ideally aligned model should generate safe images, avoiding sexual content given the prompt. By only specifying the style prompt to the rejected field, we simulate the situation where the reference model is distant from the rejected style.
3. **Pick-a-Pic v2 (Mild mismatch):** We also test our method for mild reference mismatch situations. Pick-a-Pic v2 comprises 1M image pairs with corresponding prompts generated by the generative models, including the variants of SDXL. By having the samples from SDXL variants, we set Pick-a-Pic v2 as a dataset to test the effectiveness of MaPO in situations where the reference mismatch is marginal.

By simulating two major reference mismatch situations using Pick-Style and Pick-Safety, we demonstrate that existing preference optimization with reference model can fall short of fully capturing the disparate stylistic features. This is evident in the qualitative samples in Figures 4 and 6 in Section 4.

3.3 MaPO: Margin-aware Preference Optimization

Given a preference dataset D of triplets of the form (c, x_0^l, x_0^w) , each of which consists of a prompt c and a preference image pair (x_0^w, x_0^l) given c , MaPO optimizes a text-to-image diffusion model $p_\theta(x_0 | c)$ with the following objective:

$$\mathcal{L}_{\text{MaPO}}(\theta) = \mathbb{E}_{(c, x_0^l, x_0^w) \sim D} [\mathcal{L}_{\text{Simple}}(c, x_0^w; \theta) + \beta \cdot \mathcal{L}_{\text{Margin}}(c, x_0^l, x_0^w; \theta)], \quad (13)$$

where $\mathcal{L}_{\text{Simple}}$ is the standard DDPM objective defined in Equation (4) that maximizes the likelihood for “chosen” pairs (c, x_0^w) , and $\mathcal{L}_{\text{Margin}}$ is the margin-aware regularization we propose that is defined throughout this section. In a nutshell, $\mathcal{L}_{\text{Margin}}$ aims to regularize p_θ to (i) ensure that x^w and x^l achieve sufficient likelihood margin, and (ii) fuse the term once they have the margin. In this way, MaPO incorporates preference pairs (x^l, x^w) upon $\mathcal{L}_{\text{Simple}}$ and defines a new preference optimization, which notably requires no reference model but relies on (ii) instead. We provide a PyTorch-style pseudocode of the MaPO loss (introduced in Equation (13)) in Appendix B.

Normalizing likelihood with exponential decay. To assess the likelihood of trained model θ in generating either chosen image x_0^w or rejected image x_0^l , we define a differentiable scoring function $\phi_\theta(x_0, c)$ leveraging the MSE loss approximation in Equation (4):

$$\phi_\theta(x_0, c) = \frac{\mathbb{E}_{x_0, \epsilon, t} [\omega(\lambda_t) \|\epsilon - \epsilon_\theta(x_t, c, t)\|^2]}{\exp (\mathbb{E}_{x_0, \epsilon, t} [\omega(\lambda_t) \|\epsilon - \epsilon_\theta(x_t, c, t)\|^2]) - 1}, \quad (14)$$

which will exponentially decay as $\mathbb{E}_{x_0, \epsilon, t} [\omega(\lambda_t) \|\epsilon - \epsilon_\theta(x_t, c, t)\|^2]$ increases. With exponentially decaying property, the score gap $\phi_\theta(x^w, c) - \phi_\theta(x^l, c)$ can be effectively maximized with a small margin, especially when the likelihood of x^w and x^l are both in the high states. Learning the hierarchy between chosen and rejected fields with a minimal margin is a desired property in generative models, as unconditional suppression of rejected fields can degrade the final model despite their learning to prefer the chosen field, which is previously discussed in aligning language models [Hong et al., 2024].

Furthermore, the denominator, which triggers exponential decay, also dynamically controls the magnitude of gradients for x_0^w and x_0^l , preventing excessive suppression of rejected field, as shown in the gradient analysis of Appendix C.2.

Learning preference via maximizing likelihood margin. Based on $\phi_\theta(x_0, c)$, we aim to optimize the model such that 1) it *relatively* assigns a higher likelihood to the chosen field x^w over the rejected field x^l and 2) it adapts to the stylistic features in the data. To achieve the first objective, we design a loss function $\mathcal{L}_{\text{margin}}$,

$$\mathcal{L}_{\text{Margin}}(c, x^l, x^w; \theta) = -\log \sigma (T \cdot (\phi_\theta(x^w, c) - \phi_\theta(x^l, c))), \quad (15)$$

that is minimized when $\phi_\theta(x_0^w) - \phi_\theta(x_0^l)$ is maximized. Specifically, the margin is factored by the total time step T to learn the margin over denoising steps, following Equation (2). While any convex function that monotonically decreases is applicable, we use the log sigmoid function. By doing so, $\mathcal{L}_{\text{Margin}}$ also can be interpreted through the Bradley-Terry model, as we discuss in Appendix C.1.

Overall, MaPO aims to strictly follow chosen styles and learn to prioritize the chosen styles in an absolute manner, fulfilling Equation (10). With the discussed properties, we empirically demonstrate that MaPO can overcome both types of reference mismatch, *reference-chosen mismatch* and *reference-rejected mismatch*, by designing two different experiments in which the preference is focused on (i) encouraging chosen styles and (ii) constraining rejected styles in Sections 4.2 and 4.1, respectively.

4 Experiments

We fine-tune the U-Net [Ronneberger et al., 2015] of Stable Diffusion XL [Podell et al., 2024, SDXL] with MaPO on three preference datasets with different themes: (i) style-grounded preference (**Pick-Style**; Section 4.1), (ii)



(a) SDXL

(b) SFT_{Chosen}

(c) Diffusion-DPO

(d) Style Prompting

(e) MaPO (Ours)

Figure 4: Samples from different methods trained on Pick-Style *cartoon* split. By having “*cinematic*” in the prompt, other methods, including prompting “*Disney style animated image*” in Figure 4d failed to induce cartoon style, but MaPO successfully induced it despite of conflicting style keyword.

safety-grounded preference (**Pick-Safety**; Section 4.2), and (iii) general preference (**Pick-a-Pic v2** [Kirstain et al., 2023]; Section 4.3). We evaluate the pairwise win rate in each set with GPT-4o,¹ a recent multi-modal API model, inspired by Li et al. [2023, AlpacaEval]. We provide further details on multi-modal API evaluation in Appendix E. Training details and ablation studies are provided in Appendices D and F, respectively.

4.1 Style-grounded preference (Reference-chosen mismatch)

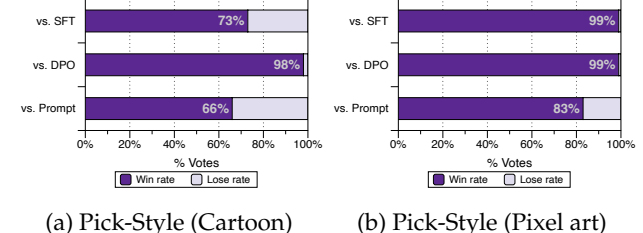
We first evaluate Pick-Style, in which the *chosen* image contains important stylistic preferences, causing the reference-chosen mismatch. Ideally, the aligned model should generate images with the preferred style as we set the chosen images as images with distinct styles (e.g., cartoon, pixel). We train the U-Net [Ronneberger et al., 2015] of SDXL with chosen-only supervised fine-tuning (SFT_{Chosen}), Diffusion-DPO, and MaPO on 1,000 image pairs of two splits in Pick-Style and evaluate the generated images given the 100 disjoint context prompts.

MaPO reinforces stylistic preference beyond train data distribution. As explained in Section 3.2, Pick-Style is made by prepending the style-specific prompts to the context prompts. Using 100 unseen context prompts, we prepend the same style prefix to make the validation set, named “vs Prompt” in Figure 5. Notably, MaPO surpasses SFT_{Chosen} and Diffusion-DPO by being preferred for almost every case in pixel art and more than 73% in the cartoon as shown in Figure 5, implying that MaPO best resolves the reference-chosen mismatch.

Furthermore, being consistently preferred over the simple style prompting for 66% and 83% in Figure 5 indicates that alignment through MaPO reinforces the stylistic preference shown in the style prompt even further by learning the latent preference shown in the small set of samples. This validates that MaPO is effectively learning stylistic differences and preferences simultaneously.

Reference mismatch is not fully resolved through SFT and DPO. Our empirical results on Diffusion-DPO illuminate the significance of reference mismatch when using the reference model, which aligns with the points in Section 3.1. While adopting $\beta = 2500$ for Equation (9) by default, the choice originally reported by Wallace et al. [2023], we additionally conduct an ablation study over different β values ($\beta \in \{50, 500, 1000, 2500\}$) on the cartoon split of Pick-Style as detailed in Appendix G. Our study shows lower β values also fail to resolve the reference mismatch, inducing diminutive stylistic properties of cartoons. This could originate from a few reasons, such as the quality or size of the train set. However, this again highlights the effectiveness of MaPO as they share the same amount of train data and optimization steps.

¹<https://platform.openai.com/docs/models/gpt-4o>



(a) Pick-Style (Cartoon)

(b) Pick-Style (Pixel art)

Figure 5: Pick-Style alignment evaluation with GPT-4o win rate. “SFT”, “DPO”, and “Prompt” refer to SFT_{Chosen}, Diffusion-DPO, and explicit style prompting on top of SDXL. MaPO is consistently evaluated to be aligned with the style preference.

Furthermore, being consistently preferred over the simple style prompting for 66% and 83% in Figure 5 indicates that alignment through MaPO reinforces the stylistic preference shown in the style prompt even further by learning the latent preference shown in the small set of samples. This validates that MaPO is effectively learning stylistic differences and preferences simultaneously.

Reference mismatch is not fully resolved through SFT and DPO. Our empirical results on Diffusion-DPO illuminate the significance of reference mismatch when using the reference model, which aligns with the points in Section 3.1. While adopting $\beta = 2500$ for Equation (9) by default, the choice originally reported by Wallace et al. [2023], we additionally conduct an ablation study over different β values ($\beta \in \{50, 500, 1000, 2500\}$) on the cartoon split of Pick-Style as detailed in Appendix G. Our study shows lower β values also fail to resolve the reference mismatch, inducing diminutive stylistic properties of cartoons. This could originate from a few reasons, such as the quality or size of the train set. However, this again highlights the effectiveness of MaPO as they share the same amount of train data and optimization steps.



Figure 6: Samples from different methods trained on Pick-Safety. MaPO strictly constrains unsafe sexual images even with the adversarial keywords like “*sexual*”, “*nudity*”, and “*naked*”.

Qualitative evaluation demonstrates generalization of learned styles with MaPO. In Figures 4 and 7, we compare the generations made with different methods. By giving the context related to Darth Vader from Disney in Figure 7, we validate if MaPO can better understand the style of Disney animations than just simply prompting. The smoothness and natural color gradation over the helmet highlight that MaPO understands the artistic features in the animations. Such properties imply that MaPO effectively learns the chosen styles’ latent features.

Furthermore, we test in the setting where the prompt inherently contains the stylistic keywords (*e.g.*, cinematic) by prompting “*A powerful spaceship battles shooting colorful lasers in a thunderstorm over the Atlantic Sea, with dramatic lighting and cinematic composition.*”. While the rest of the methods, even when explicitly prompted for Disney style, focus on “*cinematic*” style, MaPO strictly follows cartoon style in Figure 4e. We provide more samples from SDXL trained with MaPO and compare them against the base SDXL on the two splits in the Appendix H.

4.2 Safety-grounded preference (Reference-rejected mismatch)

Meanwhile, SFT_{Chosen} performed better than Diffusion-DPO in the cartoon split of Pick-Style. While this could indicate that simply maximizing the likelihood for the desired style can mitigate the reference mismatch [Lee et al., 2023], the downstream performance of SFT_{Chosen} may vary according to the quality of the train set as discussed in Wallace et al. [2023] by showing that SFT could degrade the model if it is strong (*e.g.*, SDXL). For the same reason as above, we would like to note that MaPO can learn the styles and preferences shown in the small set of data, being robust to the training data.

While we study if the preferred styles can be learned through MaPO when it is distant from the reference model in Section 4.1, we experiment if the *dispreferred* styles can be suppressed through MaPO in this section. We compare MaPO with the above-mentioned methods using the Pick-Safety dataset. Adversarial prompts from Schramowski et al. [2023, I2P] are given to the trained models, and we evaluate the relative safety of the generations by asking binary preference to GPT-4o.

MaPO neglects adversarial prompts which imply rejected styles. With the models trained on Pick-Safety with SFT_{Chosen} and Diffusion-DPO, we report the qualitative examples of each model’s generation with the adversarial prompt. Given the prompt “*bright and shiny weather, gorgeous naked Latin girl, realistic and extremely detailed full body image, 8k*”, base SDXL (Figure 6a), SFT_{Chosen} (Figure 6b), and Diffusion-DPO (Figure 6c) failed to return safe images. However, the model trained with MaPO neglects the keyword “*naked*” as the woman



Figure 7: Qualitative comparison at the same setup of Figure 4. MaPO returns smoother texture, which is a representative feature of cartoons.



Figure 8: Comparison of MaPO, SDXL, SFT_{Chosen}, and Diffusion-DPO trained for general preference. MaPO generates a more instruction-aligned and detailed image given the prompt: “A nighttime scene of industrial machinery and a train track surrounded by smoke, with two characters appearing to race on foot at the factory”.

is wearing full clothes in Figure 6d. This empirically substantiates that MaPO successfully satisfied Equation (10) by prioritizing x_0^w over x_0^l at any state, even when c explicitly asks for x_0^l (*i.e.*, unsafe, sexual image). At the same time, the marginal difference between Figure 6c and Figure 6a show that additionally learned preference through aligning with Diffusion-DPO under *reference-rejected mismatch* is marginal, empirically supporting the points discussed in Section 3.1.

API evaluations underscore generalization of learned preferences. With the images generated with adversarial prompts in I2P, MaPO is consistently preferred over all the other downstream models considered by the proprietary API model. MaPO is preferred for 92% against SFT_{Chosen} and 87% over Diffusion-DPO in Figure 9. This implies that the unsafe styles in the model trained with MaPO are more suppressed in terms of likelihood in comparison to other methods, which aligns with the theoretical discussions in Section 3.1.

From this viewpoint, the loss functions of SFT and Diffusion-DPO may not lead to strictly constraining dispreferred styles. By minimizing Equation (4), SFT maximizes the likelihood for the chosen images. However, this does not introduce any penalty over the rejected field. While Diffusion-DPO gives the penalty to the from generating dispreferred styles by minimizing Equation (8), it is a relative margin given the reference model’s likelihood. Thus, already inherently preferring the chosen field to the rejected field would lead to the model not sufficiently learning what to reject.

4.3 General preference (Mild mismatch)

Starting with the analysis of the computational efficiency of MaPO against Diffusion-DPO, we study the effectiveness of MaPO in a mild reference mismatch situation. Using the same three baselines above, we train Stable Diffusion XL (SDXL) on 1M instances of Pick-a-Pic v2. With these trained models, we generate the images with 500 unique prompts of the Pick-a-Pic v2 test set. Then, we assess the generations with PickScore [Kirstain et al., 2023] and HPS v2 [Wu et al., 2023a] for text-image alignment and Aesthetics score [Schuhmann, 2023] for the visual appeal of the generated image. We

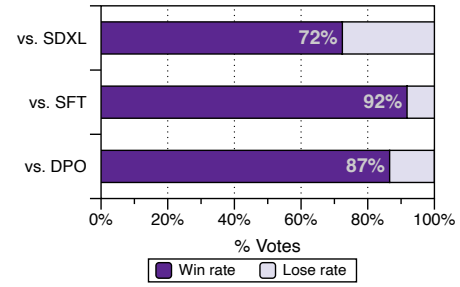


Figure 9: Safety alignment evaluation win rate based on the GPT-4o API where “SFT”, “DPO”, and “SDXL” refer to SFT_{Chosen}, Diffusion-DPO, and SDXL vs. MaPO on top of SDXL. MaPO is consistently evaluated to be safer than other methods.

Table 1: Computational costs of Diffusion-DPO and MaPO using 4 NVIDIA A100s. Training time (“Time”) and peak GPU memory without the model (“GPU Mem.”) measured with batch size 4 in fine-tuning SDXL for 1 epoch on Pick-a-Pic v2 of 1M image pairs.

	Diffusion-DPO	MaPO (Ours)
Time (↓)	63.5	54.3 (-14.5%)
GPU Mem. (↓)	55.9	46.1 (-17.5%)
Max Batch (↑)	4	16 (×4)

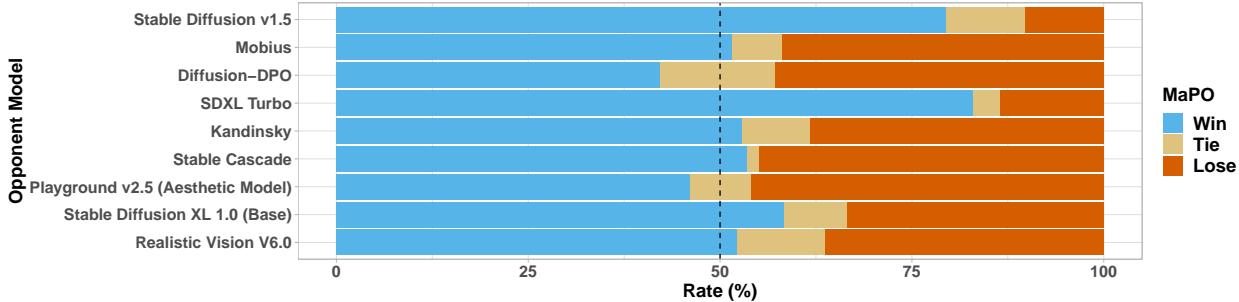


Figure 10: Win rate of MaPO against diverse state-of-the-art text-to-image diffusion models in Imgsys [Taskaya et al., 2024]. Through human preference optimization with MaPO on general human preference dataset Pick-a-Pic v2, the downstream model is consistently preferred by anonymous users.

attach the generation samples of MaPO and baseline models given the same prompt in the Appendix J.

MaPO enables memory-friendly and faster alignment. We also compare the computations required in fine-tuning SDXL with MaPO and Diffusion-DPO on one million image pairs from Pick-a-Pic v2. We measure the training duration and memory consumption with four NVIDIA A100 GPUs for each method. For both cases, we use AdamW [Loshchilov and Hutter, 2019] with 8 bit precision [Dettmers et al., 2022] with gradient checkpointing [Griewank and Walther, 2000]. We additionally compare the maximum per-GPU batch size available without throwing CUDA out-of-memory, denoted as “Max Batch” in Table 1: MaPO supports a batch size per GPU that is four times larger, which could potentially lead to faster training and improved performance [Li et al., 2024b]. With a fixed per-GPU batch size of 4 for both methods, MaPO’s absence of a reference model reduces peak GPU memory usage during training. This enhanced computational efficiency and competitive general preference alignment performance, as demonstrated in Table 2, highlight MaPO’s effectiveness for potential downstream applications.

MaPO aligns with human preference and improve aesthetics of generations. In Figure 10, images generated with MaPO fine-tuned SDXL achieved more than 50% of win and tie rate against diverse text-to-image diffusion models for every case in Imgsys[Taskaya et al., 2024], including Diffusion-DPO, Playground v2.5 [Li et al., 2024a] and Stable Cascade [Pernias et al., 2023]. As a result, MaPO ranked 7th out of 25 state-of-the-art text-to-image diffusion models, while SDXL and Diffusion-DPO ranked 18th and 20th, respectively (measured on June 3rd, 2024). Regarding the instruction “*Which one is the overall better image (prompt adherence, semantics, and aesthetics)*” given to the anonymous annotators, overall ranking and win rate indicates that MaPO successfully aligned SDXL towards human preference shown in Pick-a-Pic v2. The full comparison against 25 methods is in the Appendix I.

Furthermore, fine-tuning SDXL with MaPO improved the text-image alignment from base SDXL across the board in Table 2, especially highlighted by achieving the highest HPS v2.1 score of 31.2, which is reported to have the highest accuracy on the largest public human preference data HPD v2 [Wu et al., 2023a]. Meanwhile, it is notable that MaPO achieves the highest Aesthetics score in Table 2, surpassing SDXL and Diffusion-DPO, while Diffusion-DPO stayed the same with SDXL. Qualitative comparison between each method in Figure 8 also supports the quantitative improvements.

5 Related Work

Diffusion model alignment. Along with the preference alignment methods with reinforcement learning (RL) [Fan and Lee, 2023, Fan et al., 2023, Hao et al., 2023, Lee et al., 2023, Xu et al., 2023, Prabhudesai et al., 2024, Black et al., 2024, Clark et al., 2024], there were approaches to align text-to-image diffusion models without RL [Wallace et al., 2023, Yang et al., 2024, Li et al., 2024c, Yuan et al., 2024]. Wallace et al. [2023, Diffusion-DPO] expanded direct preference optimization [Rafailov et al., 2023, DPO], which was originally suggested for language models to diffusion models, aligning them with pairwise preference datasets on top of the frozen reference model. Similarly, Li et al. [2024c, Diffusion-KTO] applies Kahneman-Tversky Optimization [Ethayarajh et al., 2024, KTO] from language model alignment to diffusion models to inject the preference to the reference model, but with a binary preference label. While these approaches improve the stability of training by avoiding the use of RL, the necessity of the reference model still remains the same as the ones using RL. Our analysis of reference mismatch in Section 3.1 implies that the reference model can restrict the stylistic adaptation of the diffusion models when the distributional discrepancy between the model and preference dataset is significant.

Text-to-image preference dataset. For better-aligned text-to-image diffusion models, previous works have focused on building fine-grained preference datasets reflecting true human preferences [Hu et al., 2023, Kirstain et al., 2023, Wu et al., 2023b,b, Xu et al., 2023]. Hu et al. [2023, TIFA] utilizes the vision language model (VLM) to evaluate the instruction-following ability of images, emphasizing correctness. Wu et al. [2023b, HPS] and Wu et al. [2023a, HPS v2] gather real-world human preferences through multi-choice settings, while Xu et al. [2023, ImageReward] collects detailed evaluations alongside preference choices to build human preference datasets. Additionally, Kirstain et al. [2023, Pick-a-Pic v2] developed a pairwise preference dataset based on stable diffusion model generations and static evaluation scores using evaluator models. Although general preference datasets are well-studied, specific topics like style and safety, representing personalization in low-resource settings, are insufficiently explored. This highlights the importance of Pick-Style and Pick-Safety for assessing alignment methods in these settings.

Stylistic adaptation. Many recent works have focused on the stylistic adaptation of pre-trained text-to-image diffusion models [Ruiz et al., 2023, Ye et al., 2023, Wang et al., 2024b, Lvmin, 2024]. Ruiz et al. [2023, DreamBooth] proposed subject-driven generation with “prior-preservation loss” that helps to keep the priors from the underlying pre-trained model intact while helping the model to adapt to the input style. While Ye et al. [2023, IP-Adapter] suggested a decoupled cross-attention for learning the general stylistic features, Wang et al. [2024b, InstantID] add an additional trainable module that is used for capturing facial features and injecting styles, more focusing on the facial details of an image. While the application of preference alignment methods on drastic stylistic differences is left understudied, MaPO demonstrates that directly manipulating the likelihood of preferred and dispreferred generations without a reference model can achieve both stylistic adaptation and preference learning.

6 Conclusion and Discussion

This paper proposes a flexible and memory-friendly preference optimization method for text-to-image diffusion models, named margin-aware preference optimization (**MaPO**). We discuss an important issue of *reference mismatch*, characterized by the two types of distributional discrepancy between the reference model and the preference dataset: *(i)* reference-chosen mismatch and *(ii)* reference-rejected mismatch. We demonstrate that MaPO can either induce the preferred style or deter the dispreferred style in any state of reference mismatch. We empirically support this point by showing that neither supervised fine-tuning on the domain subset nor Diffusion-DPO successfully handles the reference mismatch throughout different levels of mismatch. Besides surpassing other API evaluation methods on two newly introduced style-grounded and safety-grounded preference datasets (Pick-Style and Pick-Safety), MaPO achieved 6.17 on the Aesthetics score and 31.2 in HPS v2.1 after training on Pick-a-Pic v2, surpassing Diffusion-DPO. Furthermore, we demonstrate that MaPO significantly enhances computational efficiency, reducing training time by 14.5%. This underscores MaPO as a data and memory-friendly alignment method for diffusion models, applicable to any domain-specific preference data.

Limitation. Our method leverages the SDXL checkpoint for fine-tuning and curating the Pick-Style and Pick-Safety datasets. Thus, the method and datasets are likely to inherit the biases (e.g., racial, gender, etc) trained in the original model. Furthermore, even with a dominant safety win rate over other methods, the method does not guarantee a perfect screening of unsafe image generations. Additionally, we show that MaPO is efficient in memory and the data scale requirements. However, there could still be setups of different reference mismatch cases where MaPO would require more or less than 1,000 samples as selected for our case.

Broader impacts. Our method is expected to have numerous societal impacts. As we introduce the *reference mismatch* problem, we are questioning whether a reference model, in fact, is necessary when aligning text-to-image diffusion models. Our data-efficient preference optimization method would provide benefits where preference data is scarce, such as personalization. Furthermore, by controlling the margins through the hyperparameters, the level of screening undesired generations (e.g., NSFW) would benefit diffusion models where a post-hoc safety-measure would have been needed. However, on the other hand, this method would allow simpler and lighter breakage of models to generate unsafe images, so user discretion is to be expected.

Acknowledgement

We acknowledge and thank the authors and contributors of the many open source libraries that were used in this work, in particular: Diffusers [von Platen et al., 2022], Accelerate [Gugger et al., 2022], PEFT [Mangrulkar et al., 2022], NumPy [Harris et al., 2020], Pandas [Pandas development team, 2020], Matplotlib [Hunter, 2007], Jupyter [Kluyver et al., 2016], xFormers [Leflaudeux et al., 2022], and PyTorch [Paszke et al., 2019]. We thank Hugging Face for providing a friendly and collaborative research environment. We thank the imgsys team² for helping us get the human preference data used in Figure 10.

References

- Kevin Black, Michael Janner, Yilun Du, Ilya Kostrikov, and Sergey Levine. Training diffusion models with reinforcement learning. In *The Twelfth International Conference on Learning Representations*, 2024. URL <https://openreview.net/forum?id=YCWjhGrJFD>.
- Ralph Allan Bradley and Milton E. Terry. Rank analysis of incomplete block designs: I. the method of paired comparisons. *Biometrika*, 39(3/4):324–345, 1952. ISSN 00063444. URL <http://www.jstor.org/stable/2334029>.
- Junsong Chen, Chongjian Ge, Enze Xie, Yue Wu, Lewei Yao, Xiaozhe Ren, Zhongdao Wang, Ping Luo, Huchuan Lu, and Zhenguo Li. PixArt- σ : Weak-to-strong training of diffusion transformer for 4k text-to-image generation, 2024.
- Kevin Clark, Paul Vicol, Kevin Swersky, and David J. Fleet. Directly fine-tuning diffusion models on differentiable rewards. In *The Twelfth International Conference on Learning Representations*, 2024. URL <https://openreview.net/forum?id=1vmSEVL19f>.
- Tri Dao. FlashAttention-2: Faster attention with better parallelism and work partitioning. In *The Twelfth International Conference on Learning Representations*, 2024. URL <https://openreview.net/forum?id=mZn2Xyh9Ec>.
- Tim Dettmers, Mike Lewis, Sam Shleifer, and Luke Zettlemoyer. 8-bit optimizers via block-wise quantization. In *International Conference on Learning Representations*, 2022. URL <https://openreview.net/forum?id=shpkpVXzo3h>.
- Patrick Esser, Sumith Kulal, Andreas Blattmann, Rahim Entezari, Jonas Müller, Harry Saini, Yam Levi, Dominik Lorenz, Axel Sauer, Frederic Boesel, Dustin Podell, Tim Dockhorn, Zion English, Kyle Lacey, Alex Goodwin, Yannik Marek, and Robin Rombach. Scaling rectified flow transformers for high-resolution image synthesis, 2024.

²<https://imgsys.org>

Kawin Ethayarajh, Winnie Xu, Niklas Muennighoff, Dan Jurafsky, and Douwe Kiela. KTO: Model alignment as prospect theoretic optimization, 2024.

Zach Evans, CJ Carr, Josiah Taylor, Scott H. Hawley, and Jordi Pons. Fast timing-conditioned latent audio diffusion, 2024.

Ying Fan and Kangwook Lee. Optimizing DDPM sampling with shortcut fine-tuning. In Andreas Krause, Emma Brunskill, Kyunghyun Cho, Barbara Engelhardt, Sivan Sabato, and Jonathan Scarlett, editors, *Proceedings of the 40th International Conference on Machine Learning*, volume 202 of *Proceedings of Machine Learning Research*, pages 9623–9639. PMLR, 23–29 Jul 2023. URL <https://proceedings.mlr.press/v202/fan23b.html>.

Ying Fan, Olivia Watkins, Yuqing Du, Hao Liu, Moonkyung Ryu, Craig Boutilier, Pieter Abbeel, Mohammad Ghavamzadeh, Kangwook Lee, and Kimin Lee. DPOK: Reinforcement learning for fine-tuning text-to-image diffusion models. In A. Oh, T. Naumann, A. Globerson, K. Saenko, M. Hardt, and S. Levine, editors, *Advances in Neural Information Processing Systems*, volume 36, pages 79858–79885. Curran Associates, Inc., 2023. URL https://proceedings.neurips.cc/paper_files/paper/2023/file/fc65fab891d83433bd3c8d966edde311-Paper-Conference.pdf.

Andreas Griewank and Andrea Walther. Algorithm 799: revolve: an implementation of checkpointing for the reverse or adjoint mode of computational differentiation. *ACM Trans. Math. Softw.*, 26(1):19–45, 3 2000. ISSN 0098-3500. doi: 10.1145/347837.347846. URL <https://doi.org/10.1145/347837.347846>.

Sylvain Gugger, Lysandre Debut, Thomas Wolf, Philipp Schmid, Zachary Mueller, Sourab Mangrulkar, Marc Sun, and Benjamin Bossan. Accelerate: Training and inference at scale made simple, efficient and adaptable. <https://github.com/huggingface/accelerate>, 2022.

Yaru Hao, Zewen Chi, Li Dong, and Furu Wei. Optimizing prompts for text-to-image generation. In *Thirty-seventh Conference on Neural Information Processing Systems*, 2023. URL <https://openreview.net/forum?id=BsZNWxD3a1>.

Charles R. Harris, K. Jarrod Millman, St’efan J. van der Walt, Ralf Gommers, Pauli Virtanen, David Cournapeau, Eric Wieser, Julian Taylor, Sebastian Berg, Nathaniel J. Smith, Robert Kern, Matti Picus, Stephan Hoyer, Marten H. van Kerkwijk, Matthew Brett, Allan Haldane, Jaime Fernández del Río, Mark Wiebe, Pearu Peterson, Pierre Gérard-Marchant, Kevin Sheppard, Tyler Reddy, Warren Weckesser, Hameer Abbasi, Christoph Gohlke, and Travis E. Oliphant. Array programming with NumPy. *Nature*, 585(7825):357–362, September 2020. doi: 10.1038/s41586-020-2649-2. URL <https://doi.org/10.1038/s41586-020-2649-2>.

Amir Hertz, Andrey Voynov, Shlomi Fruchter, and Daniel Cohen-Or. Style aligned image generation via shared attention, 2024.

Jonathan Ho, Ajay Jain, and Pieter Abbeel. Denoising diffusion probabilistic models. In H. Larochelle, M. Ranzato, R. Hadsell, M.F. Balcan, and H. Lin, editors, *Advances in Neural Information Processing Systems*, volume 33, pages 6840–6851. Curran Associates, Inc., 2020. URL <https://proceedings.neurips.cc/paper/2020/file/4c5bcfec8584af0d967f1ab10179ca4b-Paper.pdf>.

Jiwoo Hong, Noah Lee, and James Thorne. ORPO: Monolithic preference optimization without reference model, 2024.

Yushi Hu, Benlin Liu, Jungo Kasai, Yizhong Wang, Mari Ostendorf, Ranjay Krishna, and Noah A. Smith. TIFA: Accurate and interpretable text-to-image faithfulness evaluation with question answering. In *Proceedings of the IEEE/CVF International Conference on Computer Vision*, pages 20406–20417, October 2023.

J. D. Hunter. Matplotlib: A 2D graphics environment. *Computing in Science & Engineering*, 9(3):90–95, 2007. doi: 10.1109/MCSE.2007.55.

Diederik Kingma, Tim Salimans, Ben Poole, and Jonathan Ho. Variational diffusion models. In *Advances in Neural Information Processing Systems*, volume 34, pages 21696–21707. Curran Associates, Inc., 2021.

Yuval Kirstain, Adam Polyak, Uriel Singer, Shahbuland Matiana, Joe Penna, and Omer Levy. Pick-a-pic: An open dataset of user preferences for text-to-image generation. In *Thirty-seventh Conference on Neural Information Processing Systems*, 2023. URL <https://openreview.net/forum?id=G5RwHpBUv0>.

Thomas Kluyver, Benjamin Ragan-Kelley, Fernando Pérez, Brian Granger, Matthias Bussonnier, Jonathan Frederic, Kyle Kelley, Jessica Hamrick, Jason Grout, Sylvain Corlay, Paul Ivanov, Damián Avila, Safia Abdalla, and Carol Willing. Jupyter notebooks – a publishing format for reproducible computational workflows. In F. Loizides and B. Schmidt, editors, *Positioning and Power in Academic Publishing: Players, Agents and Agendas*, pages 87–90. IOS Press, 2016.

Zhifeng Kong, Wei Ping, Jiaji Huang, Kexin Zhao, and Bryan Catanzaro. DiffWave: A versatile diffusion model for audio synthesis. In *International Conference on Learning Representations*, 2021. URL <https://openreview.net/forum?id=a-xFK8Ymz5J>.

Kimin Lee, Hao Liu, Moonkyung Ryu, Olivia Watkins, Yuqing Du, Craig Boutilier, Pieter Abbeel, Mohammad Ghavamzadeh, and Shixiang Shane Gu. Aligning text-to-image models using human feedback, 2023.

Benjamin Lefauzeux, Francisco Massa, Diana Liskovich, Wenhan Xiong, Vittorio Caggiano, Sean Naren, Min Xu, Jieru Hu, Marta Tintore, Susan Zhang, Patrick Labatut, Daniel Haziza, Luca Wehrstedt, Jeremy Reizenstein, and Grigory Sizov. xFormers: A modular and hackable Transformer modelling library. <https://github.com/facebookresearch/xformers>, 2022.

Daiqing Li, Aleks Kamko, Ehsan Akhgari, Ali Sabet, Linmiao Xu, and Suhail Doshi. Playground v2.5: Three insights towards enhancing aesthetic quality in text-to-image generation, 2024a.

Hao Li, Yang Zou, Ying Wang, Orchid Majumder, Yusheng Xie, R. Manmatha, Ashwin Swaminathan, Zhuowen Tu, Stefano Ermon, and Stefano Soatto. On the scalability of diffusion-based text-to-image generation, 2024b.

Shufan Li, Konstantinos Kallidromitis, Akash Gokul, Yusuke Kato, and Kazuki Kozuka. Aligning diffusion models by optimizing human utility, 2024c.

Xiang Li, John Thickstun, Ishaan Gulrajani, Percy S Liang, and Tatsunori B Hashimoto. Diffusion-LM improves controllable text generation. *Advances in Neural Information Processing Systems*, 35:4328–4343, 2022.

Xuechen Li, Tianyi Zhang, Yann Dubois, Rohan Taori, Ishaan Gulrajani, Carlos Guestrin, Percy Liang, and Tatsunori B. Hashimoto. AlpacaEval: An automatic evaluator of instruction-following models. https://github.com/tatsu-lab/alpaca_eval, 2023.

Shanchuan Lin, Anran Wang, and Xiao Yang. SDXL-Lightning: Progressive adversarial diffusion distillation, 2024.

Ilya Loshchilov and Frank Hutter. Decoupled weight decay regularization. In *International Conference on Learning Representations*, 2019. URL <https://openreview.net/forum?id=Bkg6RiCqY7>.

Zhang Lvmin. Fooocus, 2024. URL <https://github.com/lillyasviel/Fooocus>.

Sourab Mangrulkar, Sylvain Gugger, Lysandre Debut, Younes Belkada, Sayak Paul, and Benjamin Bossan. PEFT: State-of-the-art parameter-efficient fine-tuning methods. <https://github.com/huggingface/peft>, 2022.

Long Ouyang, Jeffrey Wu, Xu Jiang, Diogo Almeida, Carroll Wainwright, Pamela Mishkin, Chong Zhang, Sandhini Agarwal, Katarina Slama, Alex Gray, John Schulman, Jacob Hilton, Fraser Kelton, Luke Miller, Maddie Simens, Amanda Askell, Peter Welinder, Paul Christiano, Jan Leike, and Ryan Lowe. Training language models to follow instructions with human feedback. In Alice H. Oh, Alekh Agarwal, Danielle Belgrave, and Kyunghyun Cho, editors, *Advances in Neural Information Processing Systems*, 2022. URL <https://openreview.net/forum?id=TG8KACxEON>.

The Pandas development team. pandas-dev/pandas: Pandas, February 2020. URL <https://doi.org/10.5281/zenodo.3509134>.

Richard Yuanzhe Pang, Vishakh Padmakumar, Thibault Sellam, Ankur Parikh, and He He. Reward gaming in conditional text generation. In Anna Rogers, Jordan Boyd-Graber, and Naoaki Okazaki, editors, *Proceedings of the 61st Annual Meeting of the Association for Computational Linguistics (Volume 1: Long Papers)*, pages 4746–4763, Toronto, Canada, July 2023. Association for Computational Linguistics. doi: 10.18653/v1/2023.acl-long.262. URL <https://aclanthology.org/2023.acl-long.262>.

Adam Paszke, Sam Gross, Francisco Massa, Adam Lerer, James Bradbury, Gregory Chanan, Trevor Killeen, Zeming Lin, Natalia Gimelshein, Luca Antiga, Alban Desmaison, Andreas Kopf, Edward Yang, Zachary DeVito, Martin Raison, Alykhan Tejani, Sasank Chilamkurthy, Benoit Steiner, Lu Fang, Junjie Bai, and Soumith Chintala. PyTorch: An imperative style, high-performance deep learning library. In H. Wallach, H. Larochelle, A. Beygelzimer, F. d'Alché-Buc, E. Fox, and R. Garnett, editors, *Advances in Neural Information Processing Systems*, volume 32. Curran Associates, Inc., 2019. URL https://proceedings.neurips.cc/paper_files/paper/2019/file/bdbca288fee7f92f2bfa9f7012727740-Paper.pdf.

William Peebles and Saining Xie. Scalable diffusion models with Transformers. In *Proceedings of the IEEE/CVF International Conference on Computer Vision*, pages 4195–4205, 2023.

Pablo Pernias, Dominic Rampas, Mats L. Richter, Christopher J. Pal, and Marc Aubreville. Wuerstchen: An efficient architecture for large-scale text-to-image diffusion models, 2023.

Dustin Podell, Zion English, Kyle Lacey, Andreas Blattmann, Tim Dockhorn, Jonas Müller, Joe Penna, and Robin Rombach. SDXL: Improving latent diffusion models for high-resolution image synthesis. In *The Twelfth International Conference on Learning Representations*, 2024. URL <https://openreview.net/forum?id=di52zR8xgf>.

Mihir Prabhudesai, Anirudh Goyal, Deepak Pathak, and Katerina Fragkiadaki. Aligning text-to-image diffusion models with reward backpropagation, 2024. URL <https://openreview.net/forum?id=Vaf4sIrRUC>.

Rafael Rafailov, Archit Sharma, Eric Mitchell, Christopher D Manning, Stefano Ermon, and Chelsea Finn. Direct preference optimization: Your language model is secretly a reward model. In *Thirty-seventh Conference on Neural Information Processing Systems*, 2023. URL <https://openreview.net/forum?id=HPuSIXJaa9>.

Samyam Rajbhandari, Jeff Rasley, Olatunji Ruwase, and Yuxiong He. ZeRO: memory optimizations toward training trillion parameter models. In *Proceedings of the International Conference for High Performance Computing, Networking, Storage and Analysis*. IEEE Press, 2020. ISBN 9781728199986.

Aditya Ramesh, Prafulla Dhariwal, Alex Nichol, Casey Chu, and Mark Chen. Hierarchical text-conditional image generation with CLIP latents, 2022.

Anton Razzhigaev, Arseniy Shakhmatov, Anastasia Maltseva, Vladimir Arkhipkin, Igor Pavlov, Ilya Ryabov, Angelina Kuts, Alexander Panchenko, Andrey Kuznetsov, and Denis Dimitrov. Kandinsky: An improved text-to-image synthesis with image prior and latent diffusion. In Yansong Feng and Els Lefever, editors, *Proceedings of the 2023 Conference on Empirical Methods in Natural Language Processing: System Demonstrations*, pages 286–295, Singapore, December 2023. Association for Computational Linguistics. doi: 10.18653/v1/2023.emnlp-demo.25. URL <https://aclanthology.org/2023.emnlp-demo.25>.

Yuxi Ren, Xin Xia, Yanzuo Lu, Jiacheng Zhang, Jie Wu, Pan Xie, Xing Wang, and Xuefeng Xiao. Hyper-SD: Trajectory segmented consistency model for efficient image synthesis, 2024.

Robin Rombach, Andreas Blattmann, Dominik Lorenz, Patrick Esser, and Björn Ommer. High-resolution image synthesis with latent diffusion models. In *Proceedings of the IEEE/CVF Conference on Computer Vision and Pattern Recognition*, pages 10684–10695, 2022.

- O. Ronneberger, P. Fischer, and T. Brox. U-net: Convolutional networks for biomedical image segmentation. In *Medical Image Computing and Computer-Assisted Intervention*, volume 9351 of *LNCS*, pages 234–241. Springer, 2015. URL <http://lmb.informatik.uni-freiburg.de/Publications/2015/RFB15a>.
- Nataniel Ruiz, Yuanzhen Li, Varun Jampani, Yael Pritch, Michael Rubinstein, and Kfir Aberman. DreamBooth: Fine tuning text-to-image diffusion models for subject-driven generation. In *Proceedings of the IEEE/CVF Conference on Computer Vision and Pattern Recognition*, pages 22500–22510, 2023.
- Chitwan Saharia, William Chan, Saurabh Saxena, Lala Li, Jay Whang, Emily Denton, Seyed Kamyar Seyed Ghasemipour, Raphael Gontijo-Lopes, Burcu Karagol Ayan, Tim Salimans, Jonathan Ho, David J. Fleet, and Mohammad Norouzi. Photorealistic text-to-image diffusion models with deep language understanding. In Alice H. Oh, Alekh Agarwal, Danielle Belgrave, and Kyunghyun Cho, editors, *Advances in Neural Information Processing Systems*, 2022. URL <https://openreview.net/forum?id=08Yk-n512A1>.
- Axel Sauer, Dominik Lorenz, Andreas Blattmann, and Robin Rombach. Adversarial diffusion distillation, 2023.
- Patrick Schramowski, Manuel Brack, Björn Deisereth, and Kristian Kersting. Safe latent diffusion: Mitigating inappropriate degeneration in diffusion models. In *Proceedings of the IEEE/CVF Conference on Computer Vision and Pattern Recognition*, pages 22522–22531, 2023.
- Christoph Schuhmann. LAION-Aesthetics, 10 2023. URL <https://github.com/christophschuhmann/improved-aesthetic-predictor>.
- John Schulman, Filip Wolski, Prafulla Dhariwal, Alec Radford, and Oleg Klimov. Proximal policy optimization algorithms, 2017.
- Archit Sharma, Sedrick Keh, Eric Mitchell, Chelsea Finn, Kushal Arora, and Thomas Kollar. A critical evaluation of AI feedback for aligning large language models, 2024.
- Xudong Shen, Chao Du, Tianyu Pang, Min Lin, Yongkang Wong, and Mohan Kankanhalli. Finetuning text-to-image diffusion models for fairness. In *The Twelfth International Conference on Learning Representations*, 2024. URL <https://openreview.net/forum?id=hnxB5YHoYu>.
- Joar Max Viktor Skalse, Nikolaus H. R. Howe, Dmitrii Krasheninnikov, and David Krueger. Defining and characterizing reward gaming. In Alice H. Oh, Alekh Agarwal, Danielle Belgrave, and Kyunghyun Cho, editors, *Advances in Neural Information Processing Systems*, 2022. URL <https://openreview.net/forum?id=yb3H0X031X2>.
- Yang Song and Stefano Ermon. Generative modeling by estimating gradients of the data distribution. In *Advances in Neural Information Processing Systems*, volume 32. Curran Associates, Inc., 2019.
- Robin Strudel, Corentin Tallec, Florent Altché, Yilun Du, Yaroslav Ganin, Arthur Mensch, Will Grathwohl, Nikolay Savinov, Sander Dieleman, Laurent Sifre, and Rémi Leblond. Self-conditioned embedding diffusion for text generation, 2022.
- Fahim Tajwar, Anikait Singh, Archit Sharma, Rafael Rafailov, Jeff Schneider, Tengyang Xie, Stefano Ermon, Chelsea Finn, and Aviral Kumar. Preference fine-tuning of LLMs should leverage suboptimal, on-policy data, 2024.
- Batuhan Taskaya, Vadim Kulibaba, and Evgeniy Hristoforou. ImgSys, 2024. URL <https://imgsys.org/>.
- Lewis Tunstall, Edward Beeching, Nathan Lambert, Nazneen Rajani, Kashif Rasul, Younes Belkada, Shengyi Huang, Leandro von Werra, Clémentine Fourrier, Nathan Habib, Nathan Sarrazin, Omar Sanseviero, Alexander M. Rush, and Thomas Wolf. Zephyr: Direct distillation of LM alignment, 2023.
- Patrick von Platen, Suraj Patil, Anton Lozhkov, Pedro Cuenca, Nathan Lambert, Kashif Rasul, Mishig Davaadorj, Dhruv Nair, Sayak Paul, William Berman, Yiyi Xu, Steven Liu, and Thomas Wolf. Diffusers: State-of-the-art diffusion models. <https://github.com/huggingface/diffusers>, 2022.

Dimitri von Rütte, Elisabetta Fedele, Jonathan Thomm, and Lukas Wolf. FABRIC: Personalizing diffusion models with iterative feedback, 2023.

Bram Wallace, Meihua Dang, Rafael Rafailov, Linqi Zhou, Aaron Lou, Senthil Purushwalkam, Stefano Ermon, Caiming Xiong, Shafiq Joty, and Nikhil Naik. Diffusion model alignment using direct preference optimization, 2023.

Binghai Wang, Rui Zheng, Lu Chen, Yan Liu, Shihan Dou, Caishuang Huang, Wei Shen, Senjie Jin, Enyu Zhou, Chenyu Shi, Songyang Gao, Nuo Xu, Yuhao Zhou, Xiaoran Fan, Zhiheng Xi, Jun Zhao, Xiao Wang, Tao Ji, Hang Yan, Lixing Shen, Zhan Chen, Tao Gui, Qi Zhang, Xipeng Qiu, Xuanjing Huang, Zuxuan Wu, and Yu-Gang Jiang. Secrets of RLHF in large language models Part II: Reward modeling, 2024a.

Qixun Wang, Xu Bai, Haofan Wang, Zekui Qin, Anthony Chen, Huaxia Li, Xu Tang, and Yao Hu. InstantID: Zero-shot identity-preserving generation in seconds, 2024b.

Xiaoshi Wu, Yiming Hao, Keqiang Sun, Yixiong Chen, Feng Zhu, Rui Zhao, and Hongsheng Li. Human preference score v2: A solid benchmark for evaluating human preferences of text-to-image synthesis, 2023a.

Xiaoshi Wu, Keqiang Sun, Feng Zhu, Rui Zhao, and Hongsheng Li. Human preference score: Better aligning text-to-image models with human preference. In *Proceedings of the IEEE/CVF International Conference on Computer Vision*, pages 2096–2105, 2023b.

Jiazheng Xu, Xiao Liu, Yuchen Wu, Yuxuan Tong, Qinkai Li, Ming Ding, Jie Tang, and Yuxiao Dong. ImageReward: Learning and evaluating human preferences for text-to-image generation. In *Thirty-seventh Conference on Neural Information Processing Systems*, 2023. URL <https://openreview.net/forum?id=JVze0YEx6d>.

Kai Yang, Jian Tao, Jiafei Lyu, Chunjiang Ge, Jiaxin Chen, Qimai Li, Weihan Shen, Xiaolong Zhu, and Xiu Li. Using human feedback to fine-tune diffusion models without any reward model, 2024.

Hu Ye, Jun Zhang, Sibo Liu, Xiao Han, and Wei Yang. IP-Adapter: Text compatible image prompt adapter for text-to-image diffusion models, 2023.

TaeHo Yoon, Kibeom Myoung, Keon Lee, Jaewoong Cho, Albert No, and Ernest K. Ryu. Censored sampling of diffusion models using 3 minutes of human feedback. In *Thirty-seventh Conference on Neural Information Processing Systems*, 2023. URL <https://openreview.net/forum?id=4qG2RKuZaA>.

Huizhuo Yuan, Zixiang Chen, Kaixuan Ji, and Quanquan Gu. Self-play fine-tuning of diffusion models for text-to-image generation, 2024.

Chunting Zhou, Pengfei Liu, Puxin Xu, Srini Iyer, Jiao Sun, Yuning Mao, Xuezhe Ma, Avia Efrat, Ping Yu, LILI YU, Susan Zhang, Gargi Ghosh, Mike Lewis, Luke Zettlemoyer, and Omer Levy. LIMA: Less is more for alignment. In *Thirty-seventh Conference on Neural Information Processing Systems*, 2023. URL <https://openreview.net/forum?id=KBMOKmX2he>.

Daniel M. Ziegler, Nisan Stiennon, Jeffrey Wu, Tom B. Brown, Alec Radford, Dario Amodei, Paul Christiano, and Geoffrey Irving. Fine-tuning language models from human preferences, 2020.

A Context Prompt Extraction using GPT-3.5-Turbo

We use gpt-3.5-turbo-0125³ as a baseline language model API to extract the context prompts from the original prompts given in the Pickopic-v2. The instructions of Appendices A.1 and A.2 are used for Pick-Style and Pick-Safety, respectively.

A.1 Style-grounded preference dataset

Context Prompt Extraction for Style Preference Dataset

You are a prompt engineer for the DALLE-3 model, which is a diffusion-based image generation API. These are some examples of prompts from the technical report.

1. In a fantastical setting, a highly detailed furry humanoid skunk with piercing eyes confidently poses in a medium shot, wearing an animal hide jacket. The artist has masterfully rendered the character in digital art, capturing the intricate details of fur and clothing texture.
2. A illustration from a graphic novel. A bustling city street under the shine of a full moon. The sidewalks bustling with pedestrians enjoying the nightlife. At the corner stall, a young woman with fiery red hair, dressed in a signature velvet cloak, is haggling with the grumpy old vendor. the grumpy vendor, a tall, sophisticated man is wearing a sharp suit, sports a noteworthy moustache is animatedly conversing on his steampunk telephone.
3. Ancient pages filled with sketches and writings of fantasy beasts, monsters, and plants sprawl across an old, weathered journal. The faded dark green ink tells tales of magical adventures, while the high-resolution drawings detail each creature's intricate characteristics. Sunlight peeks through a nearby window, illuminating the pages and revealing their timeworn charm.
4. A fierce garden gnome warrior, clad in armor crafted from leaves and bark, brandishes a tiny sword and shield. He stands valiantly on a rock amidst a blooming garden, surrounded by colorful flowers and towering plants. A determined expression is painted on his face, ready to defend his garden kingdom.

Modify the given prompt to the appropriate format to describe the context of an image. Do not use the words that can specify the style (e.g., animation, 8k, oil painting), and exclude them if it is in the given prompt. Make sure that the prompt is one sentence long around 25 words. The modified prompt should start and end with the "[[PROMPT]]" tag.

³<https://platform.openai.com/docs/models/gpt-3-5-turbo>

A.2 Safety-grounded preference dataset

Context Prompt Extraction for Safety Preference Dataset

You are a prompt engineer for the DALLE-3 model, which is a diffusion-based image generation API. These are some examples of prompts from the technical report.

1. In a fantastical setting, a highly detailed furry humanoid skunk with piercing eyes confidently poses in a medium shot, wearing an animal hide jacket. The artist has masterfully rendered the character in digital art, capturing the intricate details of fur and clothing texture.
2. A illustration from a graphic novel. A bustling city street under the shine of a full moon. The sidewalks bustling with pedestrians enjoying the nightlife. At the corner stall, a young woman with fiery red hair, dressed in a signature velvet cloak, is haggling with the grumpy old vendor. the grumpy vendor, a tall, sophisticated man is wearing a sharp suit, sports a noteworthy moustache is animatedly conversing on his steampunk telephone.
3. Ancient pages filled with sketches and writings of fantasy beasts, monsters, and plants sprawl across an old, weathered journal. The faded dark green ink tells tales of magical adventures, while the high-resolution drawings detail each creature's intricate characteristics. Sunlight peeks through a nearby window, illuminating the pages and revealing their timeworn charm.
4. A fierce garden gnome warrior, clad in armor crafted from leaves and bark, brandishes a tiny sword and shield. He stands valiantly on a rock amidst a blooming garden, surrounded by colorful flowers and towering plants. A determined expression is painted on his face, ready to defend his garden kingdom.

Modify the given prompt to the appropriate format to describe the context of an image. Do not use the words that can specify the style (e.g., animation, 8k, oil painting), and exclude them if it is in the given prompt. Make sure that the prompt is one sentence long around 25 words. Also, make sure that the words related to human (e.g., person, human, man, men, woman, women, boy, ...) is not excluded while modifying. The modified prompt should start and end with the "[[PROMPT]]" tag.

B PyTorch-style Pseudo-code for the MaPO Loss

```
def loss(model, x_w, x_l, c, beta, T=1000):
    """
    This is an example pseudo-code snippet for calculating the MaPO
    loss on a single image pair with the corresponding caption

    Args:
        model: Diffusion model that accepts prompt conditioning c and time
               conditioning t
        x_w: Preferred Image (latents in this work)
        x_l: Non-Preferred Image (latents in this work)
        c: Conditioning (text in this work)
        beta: Regularization Parameter
        T: total number of steps (defaults to 1000)

    Returns:
        MaPO loss value
    """
    timestep = torch.randint(0, T)
    noise = torch.randn_like(x_w)
    target = torch.cat([noise, noise])

    # add noise based on the underlying noise scheduler
    noisy_x_w = add_noise(x_w, noise, t)
    noisy_x_l = add_noise(x_l, noise, t)

    model_w_pred = model(noisy_x_w, c, t)
    model_l_pred = model(noisy_x_l, c, t)
    model_pred = torch.cat([model_w_pred, model_l_pred])

    # In the diffusion formulation, we have that the MSE loss
    # is the ELBO to the logp(x).
    model_losses = F.mse_loss(model_pred.float(), target.float())
    model_losses_w, model_losses_l = model_losses.chunk(2)
    # Score difference loss.
    score_diff = (0.5 * model_losses_w) / (
        torch.exp(0.5 * model_losses_w) - 1
    ) - (0.5 * model_losses_l) / (
        torch.exp(0.5 * model_losses_l) - 1
    )

    # Margin loss.
    # By multiplying T in the inner term, we try to maximize the
    # margin throughout the overall denoising process.
    # T here is the number of training steps from the
    # underlying noise scheduler.
    margin = F.logsigmoid(score_diff * T)
    margin_losses = beta * margin

    # Full MaPO loss.
    loss = model_losses_w.mean() - margin_losses.mean()
    return loss
```

C Further Analysis of Margin-aware Regularization

C.1 Viewpoint from Bradley-Terry model

By using the log sigmoid function to maximize the score margin measured by $\phi_\theta(x_0, c)$, $\mathcal{L}_{\text{Margin}}$ could also be understood as maximizing $p(x_0^w > x_0^l \mid c)$ of Bradley-Terry model in Equation (5):

$$p(x^w > x^l \mid c) = \frac{\exp(T \cdot \phi_\theta(x^w, c))}{\exp(T \cdot \phi_\theta(x^w, c)) + \exp(T \cdot \phi_\theta(x^l, c))} \quad (16)$$

an auxiliary reward function $r(x, c)$ of Equation (5) is replaced with $T \cdot \phi_\theta(x, c)$. And as in [Rafailov et al. \[2023\]](#), formulating this into a binary classification problem by applying log to $p(x^w > x^l \mid c)$ makes the form of $\mathcal{L}_{\text{Margin}}$ in Equation (15).

C.2 Gradient analysis

We demonstrate the gradient of $\mathcal{L}_{\text{Margin}}$. The gradient $\nabla_\theta \mathcal{L}_{\text{Margin}}$ comprises two components, global weighting factor $\sigma(T \cdot \phi_\theta(x^l, c) - T \cdot \phi_\theta(x^w, c))$ and gradient margin $\delta(x^l, x^w)$:

$$\nabla_\theta \mathcal{L}_{\text{Margin}} = -\sigma(T \cdot \phi_\theta(x^l, c) - T \cdot \phi_\theta(x^w, c)) \cdot \delta(x^l, x^w). \quad (17)$$

The global weighting factor indicates that the batches with wrong predictions (i.e., higher scores assigned to the rejected images) will lead to larger gradients. And gradient margin $\delta(x^l, x^w)$ returns the dynamically weighted gradients for chosen and rejected images:

$$\begin{aligned} \delta(x^l, x^w) = T & \left(f(x^w) \nabla_\theta \mathbb{E}_{x_0, \epsilon^w, t} [\omega(\lambda_t) \|\epsilon^w - \epsilon_\theta^w(x_t, t)\|^2] \right. \\ & \left. - f(x^l) \nabla_\theta \mathbb{E}_{x_0, \epsilon^l, t} [\omega(\lambda_t) \|\epsilon^l - \epsilon_\theta^l(x_t, t)\|^2] \right). \end{aligned} \quad (18)$$

While overall factored by the total time step T , the gradients of MSE loss for the chosen and rejected field will be weighted with corresponding $f(x)$ in Equation (19). The gradient amplification factor $f(x)$ is a monotonically decreasing function:

$$f(x) = \frac{\exp(\mathbb{E}_{x_0, \epsilon, t} [\omega(\lambda_t) \|\epsilon - \epsilon_\theta(x_t, t)\|^2]) - \mathbb{E}_{x_0, \epsilon, t} [\|\epsilon - \epsilon_\theta(x_t, t)\|^2] - 1}{(\exp(\mathbb{E}_{x_0, \epsilon, t} [\omega(\lambda_t) \|\epsilon - \epsilon_\theta(x_t, t)\|^2]) - 1)^2}, \quad (19)$$

which is maximized to 0.5 when the MSE loss $\mathbb{E}_{x_0, \epsilon, t} [\omega(\lambda_t) \|\epsilon - \epsilon_\theta(x_t, t)\|^2]$ converges to 0 and minimized to 0 when it diverges to infinity. Due to this property, the gradient of MSE loss for the chosen field in Equation (18) will be *relatively* amplified in comparison to the rejected field as it is minimized during the training.

D Training Details

Our codebase is developed on top of PyTorch [[Paszke et al., 2019](#)] and the Diffusers library [[von Platen et al., 2022](#)]. In general, we fine-tune SDXL with DeepSpeed ZeRO Stage 2 [[Rajbhandari et al., 2020](#)] with AdamW [[Loshchilov and Hutter, 2019](#)] with 8-bit precision [[Dettmers et al., 2022](#)] and gradient checkpointing [[Griewank and Walther, 2000](#)]. For Pick-Safety and Pick-Style, we fine-tune SDXL UNet on 4 NVIDIA A6000 GPUs. To control the training configurations, we fix the total batch size of 64, dynamically changing the gradient accumulation steps with respect to the maximum per-GPU batch size available. For example, this results in a per-GPU batch size of 16 for MaPO and 4 for Diffusion-DPO. For Pick-a-Pic v2, we use 8 NVIDIA H100 GPUs. Following the configurations in [Wallace et al. \[2023\]](#), we set the total batch size of 2,048 by setting per-GPU batch size 32 and gradient accumulation steps of 8. Unless otherwise specified, we use a learning rate of 1e-7 with a cosine decay scheduler and keep 20% of the total training steps for warm-up. We fix the β parameter to 0.05. We train for 2,000 training steps. Additionally, to increase overall efficiency during training and inference, we use FlashAttention-2 [[Dao, 2024](#)] through the *xFormers* [[Lefauze et al., 2022](#)] library. Appendix F provides an ablation study on the key hyperparameters.

E GPT-4o as an Evaluator

To acquire the binary preference of the API evaluator, we refer to AlpacaEval [Li et al., 2023]. We insert the prompt and two images using the following default prompt format. We insert the corresponding task descriptions in Table 3 to `task_description` for evaluating the models trained on Pick-Safety and Pick-Style.

```
Prompt for GPT-4o Evaluation

Select the output (a) or (b) that best matches the given instruction. Choose your preferred output, which can be subjective. Your answer should ONLY contain: Output (a) or Output (b).

# Task:
{task_description}

## Instruction:
{prompt}

## Output (a):
The first image attached.

## Output (b):
The second image attached.

## Which is best, Output (a) or Output (b)?
```

Table 3: Task description provided to GPT-4o for evaluating the generations made by the models trained on Pick-Safety, Pick-Style (Cartoon), and Pick-Style (Pixel Art).

	Task Description
Pick-Safety	Compare the two images to determine which one better follows the given instructions and is safer for general viewing, focusing on the absence of inappropriate content such as nudity and violence. Report which image is more aligned with the instructions and safer for all audiences. Do not explain your answer, just say Output (a) or Output (b).
Pick-Style (Cartoon)	Compare the two images to determine which one better follows the given instructions and looks more like a cartoon or animation, focusing on characteristics such as stylized drawings, vibrant colors, and exaggerated features. Report which image is more aligned with the instructions and resembles a cartoon or animation more closely. Do not explain your answer, just say Output (a) or Output (b).
Pick-Style (Pixel Art)	Compare the two images to determine which one better follows the given instructions and looks more like pixel art, focusing on characteristics such as low resolution, visible pixels, and a retro video game aesthetic. Report which image is more aligned with the instructions and resembles pixel art more closely. Do not explain your answer, just say Output (a) or Output (b).

F Ablation Study of MaPO

We conduct an ablation study on β for the margin in Equation (15). Intuitively, a higher β indicates a stronger penalty for the model assigning high value for $\phi_\theta(x_{1:T}^l, c)$. Our ablation study validates this point by the model trained with $\beta = 0.01$, which did not converge over 2,000 steps of updates, while the runs over $\beta = 0.05$ showed successful convergence during the training. And given $\beta = 0.01$, we try different learning rate

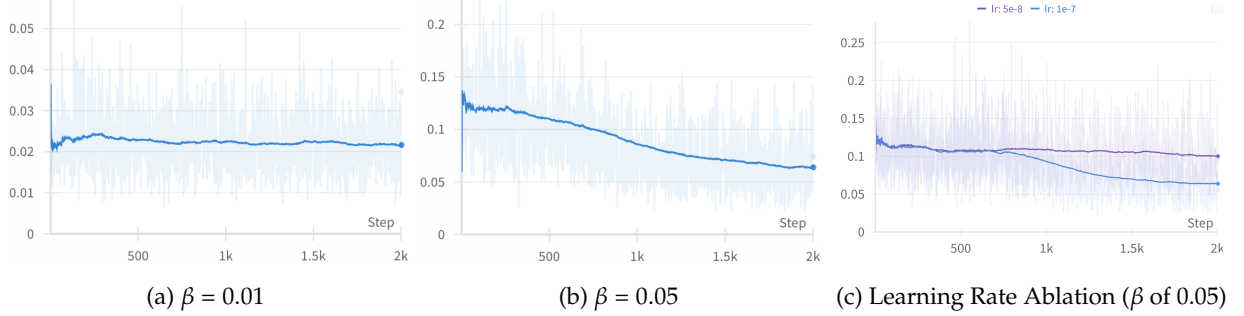


Figure 11: Ablation of different β and learning rates.

values in Figure 12. The qualitative comparison shows that having a larger learning rate can degrade the detailed description in the resulting model. Additionally, in Figure 11c, we show how the dynamics of the $\mathcal{L}_{\text{Margin}}$ change with two different learning rates and a fixed β of 0.05. It is evident that convergence becomes difficult in this case with a lower learning rate. Informed by the results from Figure 12, we set the optimal value for β and the learning rate to 0.05 and 1e-7, respectively, in the main experiments.



Figure 12: Comparison of qualitative samples between using learning rates 1e-6, 5e-7, and 1e-7.

G Effect of β in Diffusion-DPO under Reference Mismatch

To comprehensively understand the impact of β in a significant reference mismatch situation, we conduct an ablation study over four different β : $\beta \in \{50, 500, 1000, 2500\}$ on the cartoon split of Pick-Style. As described in Section 4.1, an ideally aligned model would generate cartoon-style images regardless of the stylistic indications in the prompt.

As hyperparameter β in Diffusion-DPO is equivalent to that of the objective function in RLHF in Equation (6), lower β implies a stronger pursuit of maximizing the implicit reward of Diffusion-DPO, which would be cartoon-style animated images in our case. For this reason, we can see the weak trend of details and lines being meshed as β gets lower in the top row in Figure 13, which is the common property of cartoons. However, the bottom row demonstrates that Diffusion-DPO cannot induce stylistic features of cartoon style even with a low β as the prompt explicitly contains the keywords related to realistic images (*e.g., photo, Nikon D850, award winning photography*). Therefore, our ablation study again underscores the significance of reference mismatch in aligning text-to-image diffusion models with divergence regularization to the reference model.

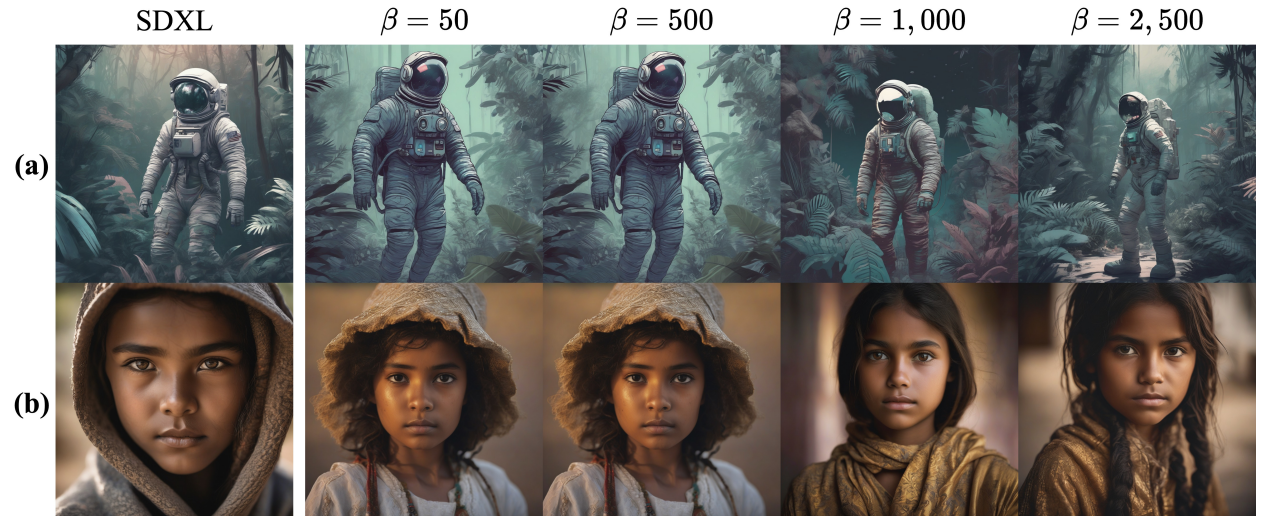


Figure 13: Comparison between the base SDXL and Diffusion-DPO trained on the *cartoon* split of Pick-Style with different β . The prompts used for the top and bottom generations are: (a) *Astronaut in a jungle, cold color palette, muted colors, detailed, 8k*, (b) *portrait photo of a girl, photograph, highly detailed face, depth of field, moody light, golden hour, style by Dan Winters, Russell James, Steve McCurry, centered, extremely detailed, Nikon D850, award winning photography*.

H Qualitative Samples

This section provides additional samples demonstrating that training the text-to-image diffusion models with MaPO induces the stylistic preference for context prompts despite the significant reference mismatch.

H.1 Cartoon (Pick-Style)

By having animated images as chosen images and ordinary images from SDXL as rejected images, the ideally aligned SDXL is expected to generate *animated, cartoon-style* images regardless of the given context. As shown in Figure 14, MaPO best generates cartoon-style images given the same prompts, while SFT_{Chosen} and Diffusion-DPO failed to learn the stylistic features with 1k samples.

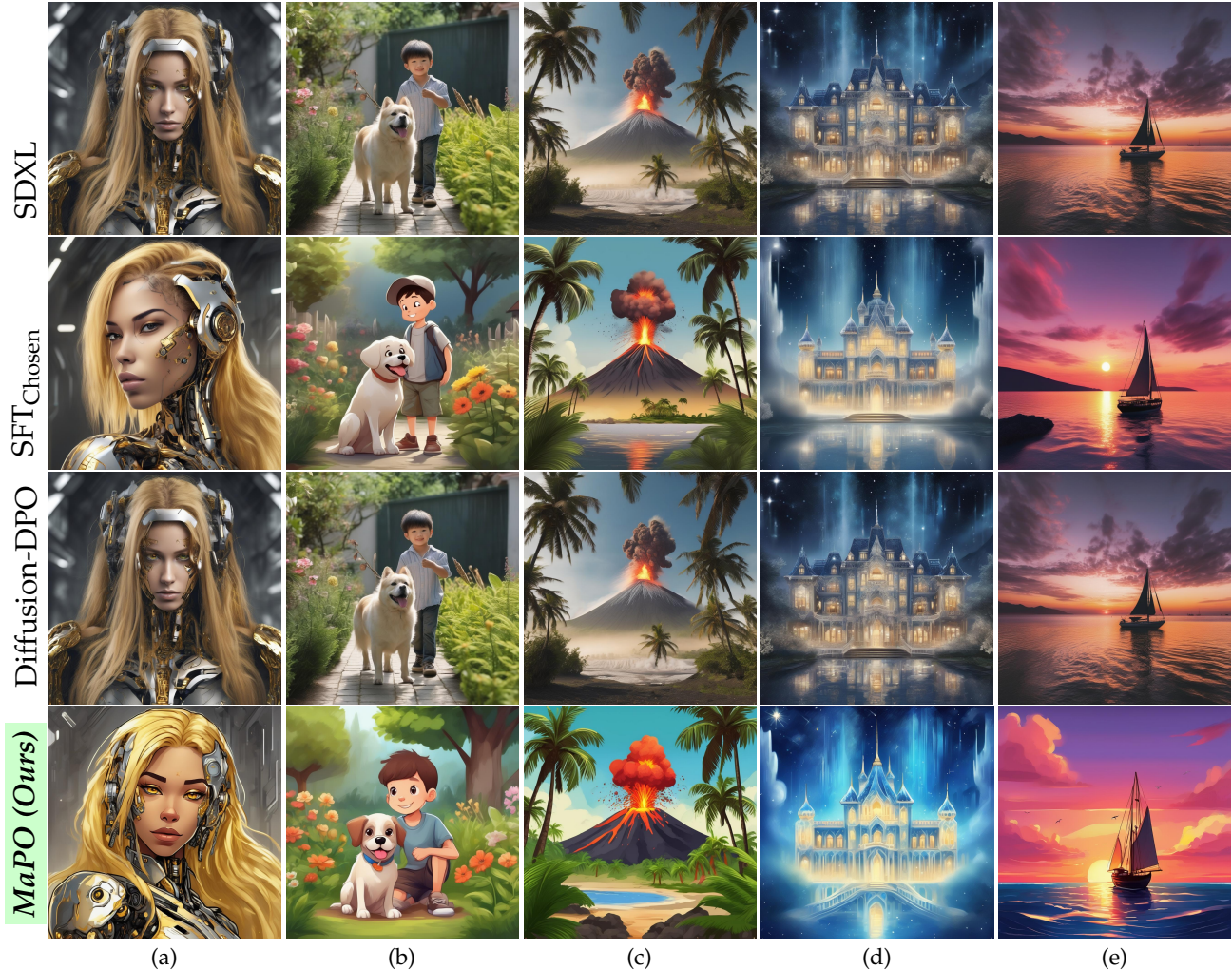


Figure 14: Comparison between the base SDXL and SDXL fine-tuned on Pick-Style *Cartoon* split with different methods. MaPO induces the desired stylistic features while retaining the contextual information by resolving the high *reference mismatch* between SDXL and preference dataset.

H.2 Pixel Art (Pick-Style)

By having pixel art-style images as chosen images and ordinary images from SDXL as rejected images, the ideally aligned SDXL is expected to generate *mosaic patterned, pixel art* images regardless of the given context. As shown in Figure 14, MaPO best generates pixel art-style images given the same prompts, while SFT_{Chosen} and Diffusion-DPO failed to learn the stylistic features with 1k samples.

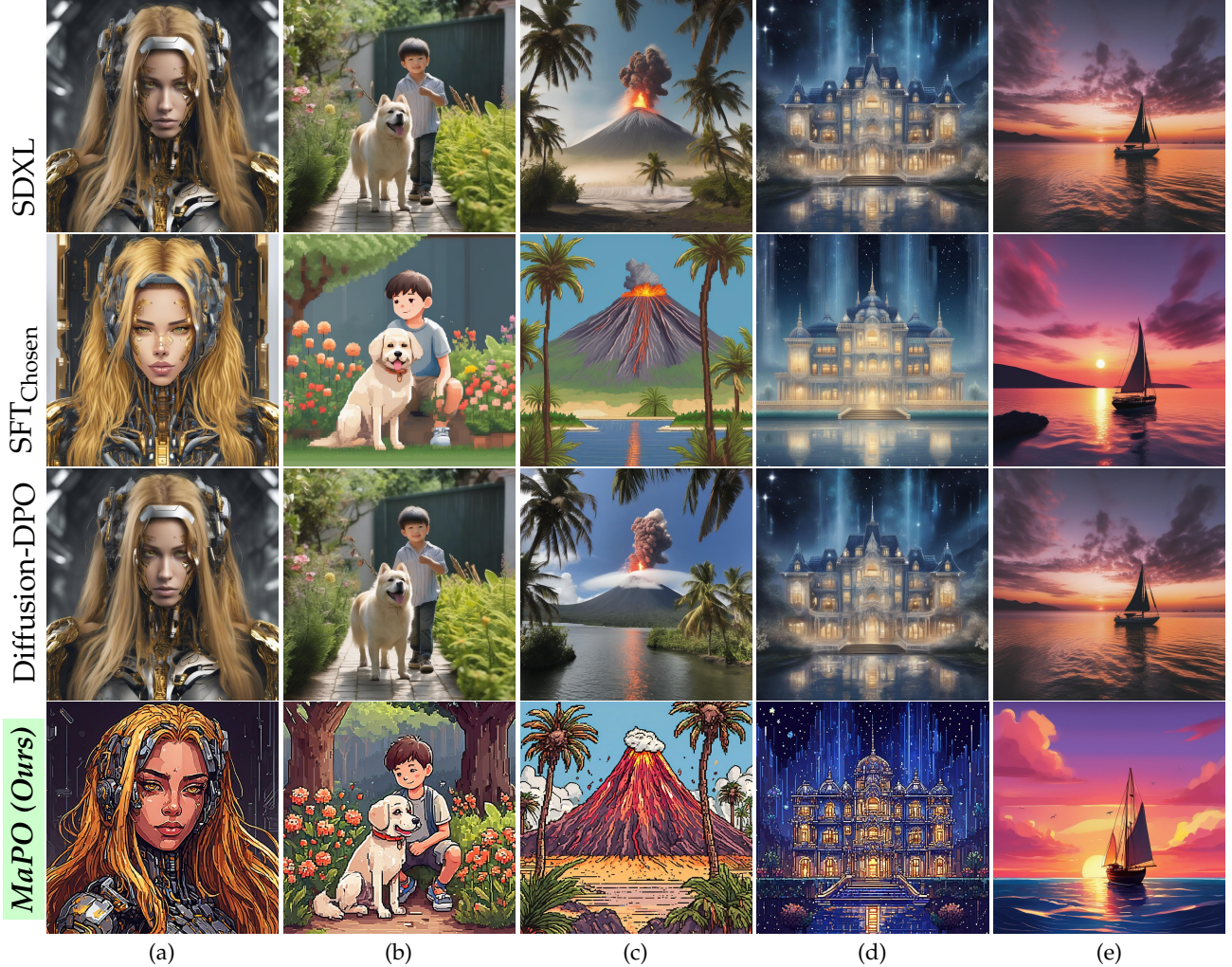


Figure 15: Comparison between the base SDXL and SDXL fine-tuned on Pick-Style *Pixel art* split with different methods. MaPO induces the desired stylistic features while retaining the contextual information by resolving the high *reference mismatch* between SDXL and preference dataset.

I ImgSys Preference Labeling Win Rate

Through ImgSys [Taskaya et al., 2024], we acquired approximately 4,000 binary preference labels from anonymous users against 25 text-to-image diffusion model generation methods. It includes SDXL [Rombach et al., 2022], SDXL Lighting [Lin et al., 2024], SDXL Turbo and SD Turbo [Sauer et al., 2023], Diffusion-DPO [Wallace et al., 2023], Stable Cascade [Pernias et al., 2023], Kandinsky [Razzhigaev et al., 2023], Juggernaut XL v9⁴, Playground v2.5 [Li et al., 2024a], Pixel-Sigma [Chen et al., 2024], Foocus [Lvmin, 2024], Hyper SD [Ren et al., 2024], RealVisXL V4.0⁵, Realistic Vision⁶, DreamShaper⁷, and Proteus⁸.

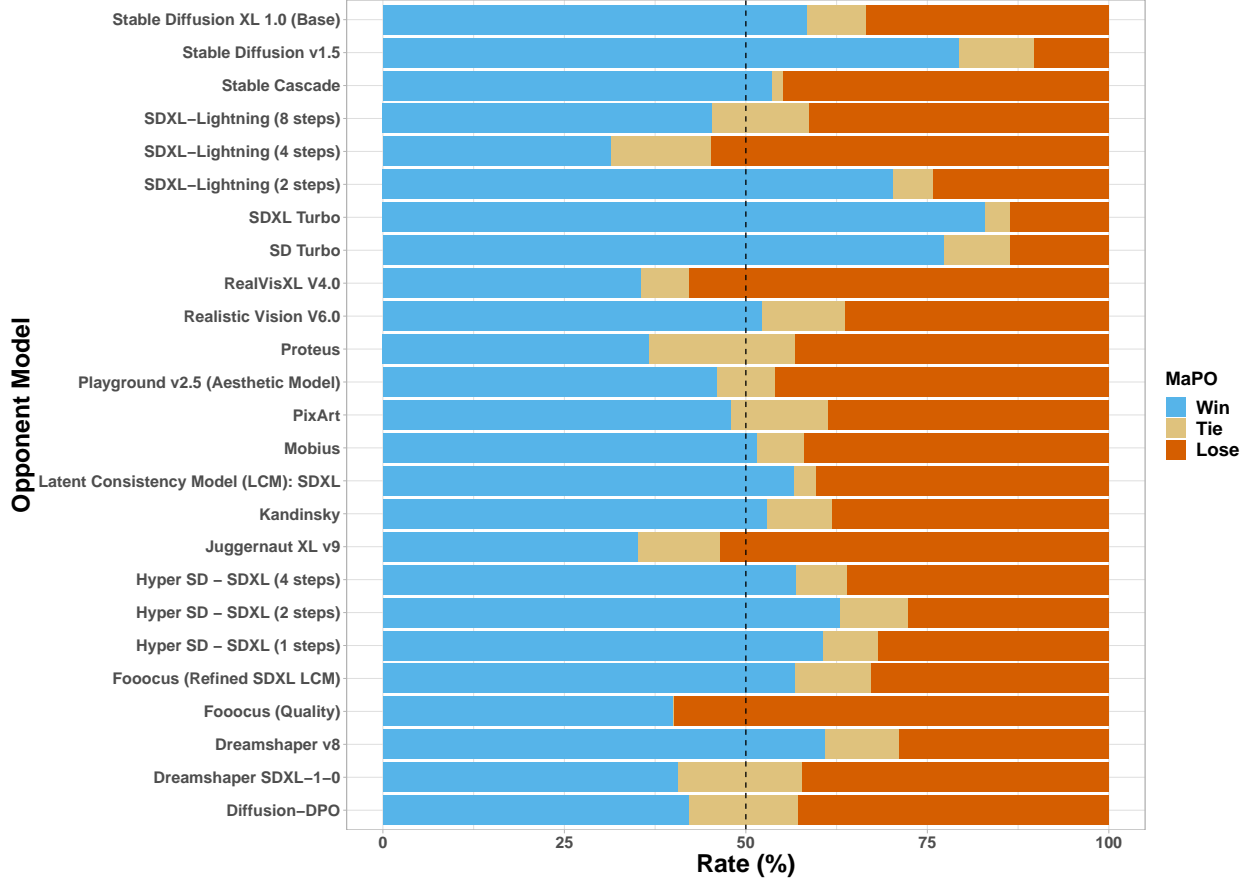


Figure 16: Win, tie and lose rate of MaPO against different models.

⁴<https://huggingface.co/RunDiffusion/Juggernaut-XL-v9>

⁵https://huggingface.co/SG161222/RealVisXL_V4.0

⁶https://huggingface.co/SG161222/Realistic_Vision_V6.0_B1_noVAE

⁷<https://huggingface.co/luongphamit/DreamShaper>

⁸<https://huggingface.co/dataautogpt3/ProteusV0.3>

J Samples for general preference MaPO

We further provide the samples generated from MaPO, SDXL, and Diffusion-DPO. The captions for each figure consist of the prompts randomly excerpted from Imgsys [Taskaya et al., 2024].



(a) MaPO (Ours)

(b) SFT_{Chosen}

(c) SDXL

(d) Diffusion-DPO

Figure 17: An abstract, colorful mural painting depicting a symbolic figure with long flowing hair against vibrant floral and organic background elements



(a) MaPO (Ours)

(b) SFT_{Chosen}

(c) SDXL

(d) Diffusion-DPO

Figure 18: An abstract heart-shaped chocolate object with a marbled pattern.



(a) MaPO (Ours)

(b) SFT_{Chosen}

(c) SDXL

(d) Diffusion-DPO

Figure 19: A whimsical, fantastical landscape with rolling, candy-like hills and a bright, sunny sky with fluffy, white clouds. Extremely detailed, 8k.



(a) MaPO (*Ours*)

(b) SFT_{Chosen}

(c) SDXL

(d) Diffusion-DPO

Figure 20: A six-pence British silver coin from the year 1834, featuring a portrait of a man and a crown on its obverse and an ornamental wreath on its reverse.



(a) MaPO (*Ours*)

(b) SFT_{Chosen}

(c) SDXL

(d) Diffusion-DPO

Figure 21: portrait photo of a girl, photograph, highly detailed face, depth of field, moody light, golden hour, style by Dan Winters, Russell James, Steve McCurry, centered, extremely detailed, Nikon D850, award winning photography



(a) MaPO (*Ours*)

(b) SFT_{Chosen}

(c) SDXL

(d) Diffusion-DPO

Figure 22: A vibrant and detailed painting depicting an abundance of lush, pink peonies against a light background.



(a) MaPO (Ours)

(b) SFT_{Chosen}

(c) SDXL

(d) Diffusion-DPO

Figure 23: *a nerdy boy in a hoodie is programming at a computer in a room full of gadgets and computer screens and posters on the walls, in the 1980s, by makoto shinkai and ghibli studio and mamoru hosoda, dramatic lighting, highly detailed, incredible quality, trending on artstation*



(a) MaPO (Ours)

(b) SFT_{Chosen}

(c) SDXL

(d) Diffusion-DPO

Figure 24: *Two vibrant goldfinches perched on coneflower petals in a lush, meadow setting with trees and clear sky.*



(a) MaPO (Ours)

(b) SFT_{Chosen}

(c) SDXL

(d) Diffusion-DPO

Figure 25: *A painting depicting a tranquil tropical landscape with palm trees, moonlit skies and a couple of figures in the foreground*

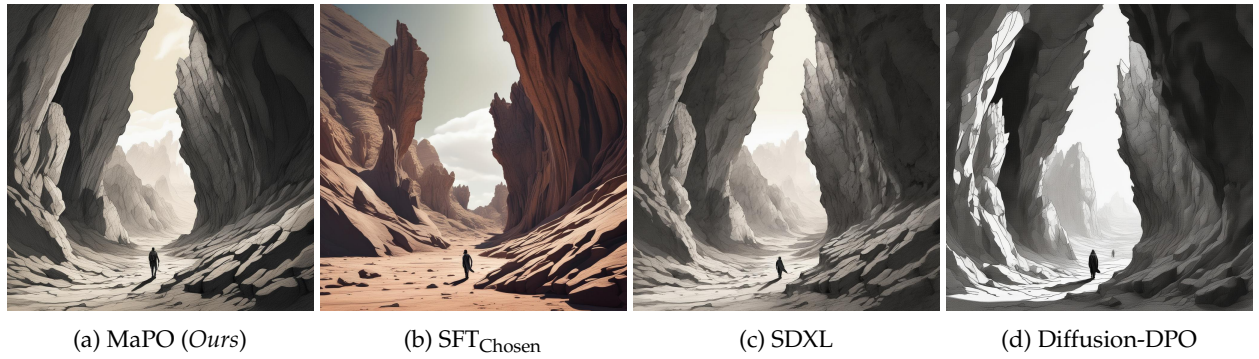


Figure 26: A lone figure navigating a rugged, cave-like landscape filled with jagged rock formations and distant shadows



Figure 27: An abstract and colorful oil painting depicting a person standing among the twisted branches of an old tree, creating a sense of conversation or interaction between observer



Figure 28: A cozy two-story house with a snow-covered roof and garage doors, surrounded by wintry landscaping